ERDC/GSL TR-21-2

US Army Corps
of Engineers®
Engineer Research and
Development Center

ERDC
ENGINEER RESEARCH & DEVELOPMENT CENTER

Rapid Airfield Damage Recovery Next Generation Backfill Technologies Comparison Experiment

Technology Comparison Experiment

Mariely Mejias-Santiago, Lyan Garcia, and Lulu Edwards

February 2021

Geotechnical and Structures Laboratory

The U.S. Army Engineer Research and Development Center (ERDC) solves the nation's toughest engineering and environmental challenges. ERDC develops innovative solutions in civil and military engineering, geospatial sciences, water resources, and environmental sciences for the Army, the Department of Defense, civilian agencies, and our nation's public good. Find out more at www.erdc.usace.army.mil.

To search for other technical reports published by ERDC, visit the ERDC online library at https://erdclibrary.on.worldcat.org/discovery.

ERDC/GSL TR-21-2
February 2021

Rapid Airfield Damage Recovery Next Generation Backfill Technologies Comparison Experiment

Technology Comparison Experiment

Mariely Mejias-Santiago, Lyan Garcia, and Lulu Edwards

Geotechnical and Structures Laboratory
U.S. Army Engineer Research and Development Center
3909 Halls Ferry Road
Vicksburg, MS 39180-6199

Final report

Prepared for Headquarters, Air Force Civil Engineer Center
Tyndall Air Force Base, FL 32403-5319

Under Project Number P246334

Abstract

The Rapid Airfield Damage Recovery (RADR) Next Generation Backfill Technology Comparison Experiment was conducted in July 2017 at the East Campus of the U.S. Army Engineer Research and Development Center (ERDC), located in Vicksburg, MS. The experiment evaluated three different crater backfill technologies to compare their performance and develop a technology trade-off analysis. The RADR next generation backfill technologies were compared to the current RADR standard backfill method of flowable fill. Results from this experiment provided useful information on technology rankings and trade-offs. This effort resulted in successful crater backfill solutions that were recommended for further end user evaluation.

Contents

Figures and Tables

Figures

Tables

Preface

This study was conducted for the U.S. Air Force Civil Engineer Center (AFCEC) under the Rapid Airfield Damage Recovery Research and Development Program, Project Number P246334. The technical monitor was Dr. Bobby Diltz, AFCEC. The Program Manager was Mr. Jeb S. Tingle.

This work was performed by the Airfields and Pavements Branch (GMA) of the Engineering Systems and Materials Division (GM), U.S. Army Engineer Research and Development Center, Geotechnical and Structures Laboratory (ERDC-GSL). At the time of publication, Ms. Anna Jordan was Chief, GMA; Mr. Justin S. Strickler was Chief, GM; and Mr. R. Nicholas Boone, CEERD-GZT, was the Technical Director for Force Projection and Maneuver Support. Mr. Charles W. Ertle II was Deputy Director of ERDC-GSL, and Mr. Bartley P. Durst was the Director.

COL Teresa A. Schlosser was the Commander of ERDC, and Dr. David W. Pittman was the Director.

1 Introduction

1.1 Background

1.1.1 Airfield Damage Repair

The airfield damage repair (ADR) process consists of engineer personnel activities in response to an attack on an airbase to provide adequate launch and recovery surfaces for the mission aircraft. Although ADR criteria are based on repairing airfields in friendly territory, recent military operations require repairing airbases occupied previously by hostile forces damaged during forcible entry or purposely sabotaged by departing forces. Legacy ADR methods for repairing bomb damage consist of using debris to fill the crater, followed by placement of crushed stone backfill with a foreign object debris (FOD) cover. ADR encompasses other areas besides the repair of bomb damage including damage assessment, identification of candidate minimum operating strips, and the safe disposal of unexploded ordnance (Department of the Army, Navy, and Air Force 2003).

In 2002, the U.S. Army Engineer Research and Development Center began the most prominent research program addressing ADR. The program included several load cart tests and flight tests that revealed none of the legacy repair technologies were capable of supporting C-17 aircraft on a runway where high, horizontal breaking forces caused the systems to fail. For C-17 operations only, the repairs can be performed without the protective mat surfacing or FOD cover. However, protective surfacing or FOD covers are required for fighter aircraft operations. Thus, the legacy repair technologies cannot be used on airfields subjected to both fighter and heavy cargo aircraft, due to the inability of the legacy repairs to sustain C-17 operations and the inability of fighter aircraft to operate on unsurfaced repairs.

During the following decade, ERDC efforts were dedicated to address the operational limitations of legacy repair methods. Research was conducted to develop capability to return damaged runways to full operational sortie production in less than 8 hr. Evaluations included new materials, tactics, techniques, and procedures (TTPs), and prototype equipment for rapid automated airfield damage assessment and crater repair (Tingle et al. 2009). Multiple operational utility assessments (OUAs) were conducted to

demonstrate the updated ADR methods and to collect feedback from the end users for further refinement as part of the Critical Runway AssessmenT and Repair (CRATR) Joint Capabilities Technology Demonstration (JCTD). Following the CRATR JCTD, multiple other troop and full-scale tests have been conducted to address other gaps identified within the scope of the Rapid Airfield Damage Recovery (RADR) modernization program. The RADR program focused on refining techniques and reducing the logistical footprint of the ADR process.

1.1.2 RADR repair tasks

The crater repair process developed during the CRATR JCTD and further refined during the RADR modernization program is well-documented in many references (Bell et al. 2013; Priddy et al. 2013; Edwards et al. 2013; Carruth et al. 2015). First, large debris is removed with compact track loaders and large front-end loaders. Next, the stanchion method is used (USAF 1992) to mark the extent of upheaval before a square repair area on the pavement is marked. The marked area is then saw-cut, followed by breaking and removal of the existing material with wheeled excavators.

Once the repair is excavated, it is backfilled, typically with rapid-setting flowable fill (Figure 1.1) or compacted crushed stone. The main purpose of the backfill is to fill the void and provide enough support to the repair cap to withstand the loads from aircraft traffic. Rapid-setting flowable fill has proven to be the best backfill alternative for RADR.

Figure 1.1. RADR backfill method of flowable fill capped with rapid-setting concrete.

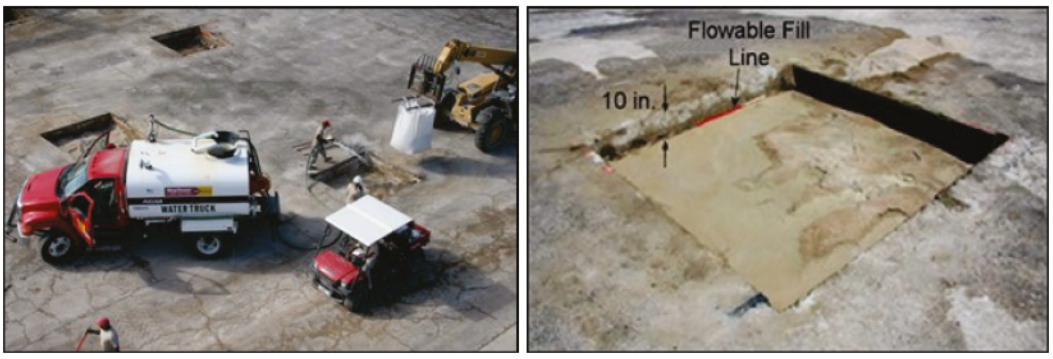

Lastly, the repair is capped with rapid-setting concrete by using the U.S. Air Force Simplified Volumetric Mixer, or with recycled asphalt cookies using a Bagela recycler and appropriate large pneumatic and steel-wheel compaction equipment.

1.1.1 Need for new backfill methods

While the current RADR crater repair method provides successful results, it is heavily dependent on specific material and equipment resources. Other repair alternatives are required in the event that large quantities of rapid-setting flowable fill and rapid-setting cement super sacks cannot be transported to the repair site. Backfill alternatives are not included in the TTPs.

Three repair alternatives for backfill that have proven their suitability for use in RADR are: 1) expandable polyurethane foam, 2) mechanical soil reinforcement, and 3) chemical soil stabilization. However, each backfill technology requires additional refinement to ultimately meet all RADR requirements. Also, there are no clear indications as to how the performance of each of these methods compares to each other.

This project consisted of evaluating the three backfill technologies in full-scale controlled test environments and comparing the performance of each technology to the standard rapid-setting flowable-fill backfill method described in the RADR TTPs.

1.1.1.1 Expandable polyurethane foam

The foam backfill technology consists of mechanically pouring liquid polyurethane foam into a crater void, then waiting for the foam to expand and set. The foam expands six times its original liquid volume; therefore, enough liquid volume is poured so that when the foam expands, it leaves room for a minimum 10-in.-thick rapid setting concrete cap. The polyurethane foam provides a uniform, low-quality backfill to support the rapid-setting concrete cap. Its primary function is to fill the crater void while providing uniform support to the rapid-setting concrete slab.

Previous research efforts and end-user demonstration exercises showed two main issues associated with this technology, i.e., (1) material sensitivity to moisture and (2) clogging of the reacted foam material within the mechanical distribution system (Priddy et al. 2013). This technology was recently refined by redesigning the foam distribution equipment, improving foam material formulations, and upgrading the foam backfill placement procedures (Figure 1.2) (Johnson et al. 2017). The refined technology was successfully demonstrated at the Silver Flag Exercise Site at Tyndall Air Force Base in 2016, where ten airmen evaluated the

technology by performing nine crater repairs and provided valuable feedback for further technology refinement (Mejias-Santiago et al. draft*).

Figure 1.2. Foam backfill demonstration.

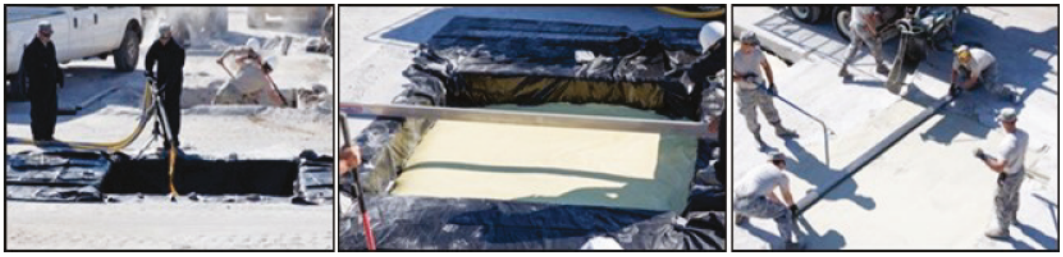

1.1.1.2 Geocell mechanical stabilization

Formerly known in the Department of Defense (DOD) community as "sand grid," geocell is a geosynthetic cellular confinement system used to reinforce geotechnical materials (Figure 1.3). Within the scope of ADR, geocells have been used to reinforce backfill materials for expedient crater repairs (Read and Dukes 1988, Webster 1986). One of the primary benefits of using geocells is that lower quality backfill materials can be used rather than the traditional well-graded crushed limestone material. This application is particularly beneficial at deployed locations where the use of indigenous materials is desired since large stockpiles of quality materials are not routinely available. At permanent installations, the use of geocells to reinforce lower quality geotechnical materials minimizes the requirement for prepositioned stockpiles of high-quality aggregates. The original TTPs for the use of geocells (sand grid) were developed in the 1980s, and the original geocell material has significantly changed. New commercial geocell products have emerged since the expiration of the original government patent, and many of the new products were evaluated against desired performance standards. In addition, the performance of different soil types reinforced with geocell for RADR missions had not been adequately quantified and documented. Investigations performed in 2016-2017 were aimed at addressing these gaps and evaluating new products with different backfill materials for selecting optimum geocell

* Mejias-Santiago, M., J. S. Tingle, J. L. Johnson, L. A. Gurtowski and C. S. Griggs. Draft. *Refinement of foam backfill technology for expedient airfield damage recovery Phase III: Technology demonstration and end user evaluation*. ERDC/GSL TR. Vicksburg, MS: U.S. Army Engineer Research and Development Center.

materials and geometries. Successful performance was observed for several products (Garcia et al. draft*).

Figure 1.3. Geocell mechanical stabilization method.

1.1.1.3 Chemically stabilized soil

The chemically stabilized soil backfill method (Figure 1.4) utilizes the locally available soil mixed with an additive, typically cement, lime, fly ash, or polymers. The soil stabilization additive(s) are used to modify the soil properties and improve strength and stiffness. Other additives include sodium silicate and polyurethane-based products. According to UFC 3-250-11, a minimum 7-day unconfined compressive strength (UCS) of 500 psi is required for a rigid pavement base course. Normally, with chemically stabilized soils, additives are placed in bulk with a truck with spreader bar or from bags. The additives are typically mixed in the soil using a rotary mixer and then compacted. However, the equipment used for traditional soil stabilization operations (i.e. highway applications) is not available or feasible for RADR scenarios. In 2017, laboratory tests were conducted to evaluate viable chemical stabilization alternatives for use in crater repairs (Johnson et al. 2018). With limited equipment available, an alternative method for mixing and compacting was fielded and proven as a reduced-logistics technology.

* Garcia, L., J. Rowland, and J. S. Tingle. Draft. *Rapid Airfield Damage Recovery Program, evaluation of geocell-reinforced backfill*. ERDC/GSL TR. Vicksburg, MS: U.S. Army Engineer Research and Development Center.

Figure 1.4. Chemically stabilized soil backfill method.

1.2 Objective

The main objective of the work presented in this report was to demonstrate three different crater repair backfill technologies under similar operational conditions and compare their performance. The technologies evaluated included (1) expandable polyurethane foam, (2) mechanical soil reinforcement, and (3) chemical soil stabilization.

1.3 Scope

The three backfill technologies were evaluated during a full-scale field experiment conducted at ERDC in Vicksburg, MS, in July 2017. The exercise consisted of repairing eight simulated craters in two days. Four craters were repaired consecutively each day, and only the backfill and capping steps of the repair procedure were conducted during this experiment for simplicity. All repairs had the same geometric characteristics, i.e., volume and layer thicknesses, as well as the same capping material to capture the relative performance of each technology and support a fair comparison between the technologies.

Simulated F-15E aircraft traffic was applied to each of the completed repairs to verify their ability to meet the operational RADR mission requirements. Detailed performance data were gathered in terms of timing, manpower requirements, and logistical requirements to support a trade-off analysis of these technologies.

2 Crater Repair Test Materials

2.1 Constructed subgrade soil

A silty clay (CL-ML) was used as the constructed subgrade material for all of the repairs. This material was purchased from a local quarry and classified according to ASTM D2487 (2017a). Classification data are shown in Appendix A.

2.2 Backfill soils

Two different backfill soils were used for the mechanical soil reinforcement and chemical soil stabilization methods. The mechanical soil reinforcement method used a poorly graded sand (SP) or a silty sand (SM) blend as the backfill materials for individual repairs. For the chemical soil stabilization methods, the SM blend was used as the backfill material. The SP was obtained from a local vendor. The SM blend was produced at ERDC by mixing 33% of ML with 67% of SP (by dry weight of total soil blend). Classification data for the SM and SP are shown in Appendix B.

2.3 Polymers

Polymer emulsions are commonly used for soil stabilization and dust control. These materials coat and physically bind soil particles together to provide stiffness, toughness, and water resistance. Previously, an in-depth study conducted at ERDC (Johnson et al. 2018) tested four products that included Soil-Sement®, GRT 9000®, Soiltac®, and Top Seal White®. According to Johnson et al. (2018), these products produced the highest 7-day UCS of the different polymers tested in the lab, ranging from 401 to 583 psi at 6% moisture content and approximately 3% to 4% polymer by dry weight of soil. Only polymers that were able to produce high strengths, i.e., UCS greater than 400 psi, at a concentration of 3% to 4% were selected for inclusion in the crater repair tests to minimize the amount required in the field. Soil stabilization with polymers is a challenge in a small crater environment because the traditional equipment used to mix polymers with soil in place, such as a soil stabilizer reclaimer, is too large for use in craters and not available for RADR.

Soil-Sement®, manufactured by Midwest Industrial Supply, is a polymer emulsion normally used for dust control and soil stabilization. Soil-Sement® was chosen for use in this experiment because of its performance

in prior field testing (Edwards draft*). Soil-Sement® produced the best results in terms of California bearing ratio (CBR) values as measured by the in-situ CBR method and with a Dynamic Cone Penetrometer (DCP).

2.4 Portland limestone cement (PLC)

Portland limestone cement (PLC) is a combination of calcium silicate-based clinker, limestone, and gypsum and is designated as Type 1L according to ASTM C595 (2019). Portland cement can be used to stabilize a variety of soil types; however, high-plasticity soils may not be as beneficial (UFC 3-250-11 2004). PLC differs from regular portland cement in that it contains more than 5% limestone and is made by grinding portland cement clinkers with limestone up to 15%. The advantage of using PLC is the reduced carbon footprint during the manufacturing process and increased hydration for cementitious efficiency (http://www.theconcreteproducer.com/how-to/concrete-production/the-advantages-of-portland-limestone-cement_0).

2.5 Geocells

The geocells used for this investigation were manufactured by Presto – Geosystems. The product, called Geoweb®, is made from high-density polyethylene (HDPE) with cell dimensions of approximately 8.8 in. × 10.2 in. and a cell height of 8 in. The specific product designation is GW20V8. Mechanical properties for the GW20V8 geocell used in this experiment are shown in Table 2.1.

* Edwards, L. Draft. *Field evaluation of next-generation backfill materials and methods for Airfield Damage Repair*. ERDC/GSL TR. Vicksburg, MS: U.S. Army Engineer Research and Development Center.

Table 2.1. GW20V8 mechanical properties.

Property	Product
Yield Strength (lb)	439
Yield Elongation (%)	9.1
UV Resistance: Yield Strength Retained (%)	95
UV Resistance: Elongation Retained (%)	98
Weld Peel Strength (lb.)	477
Weld Peel Efficiency (%)	109
Dominating Failure Mode	Failure at perforation
Weld Shear Strength (lb.)	466
Weld Shear Efficiency (%)	106
Dominating Failure Mode	Failure at perforation

2.6 Expanding polyurethane foam

Rigid polyurethane foam consists of two components, i.e., (a) polymeric isocyanate compound and (b) a blend of polyol compounds, catalysts, proprietary additives, and water. The two components are mixed in a 1:1 ratio (by volume) to form a closed-cell expanding polyurethane foam that rises and sets in approximately 15 min. The foam product used for RADR is Foam-iT! 10 Slow®, which is a water-blown, rigid polyurethane designed to expand approximately six times its initial volume to produce a final density of approximately 10 pcf. At this density, the rigid closed cell polyurethane foam produces a minimum unconfined compressive strength (UCS) of 200 psi, which is adequate to provide uniform load support for the rapid-setting concrete cap. This material is formulated with a relatively slow reaction rate for easier handling during large-pour operation.

The main benefit of using expanding polyurethane foam for crater backfill is the significant reduction in material requirements, which reduces the logistical footprint of the repair process. As shown in Figure 2.1, material reductions are such that 4,500 lb of liquid foam would replace 30,000 lb of backfill soil. This is especially important during base recovery operations in remote locations where quality backfill materials are not available and air-deployable technologies are required.

Figure 2.1. Benefits of foam expansion.

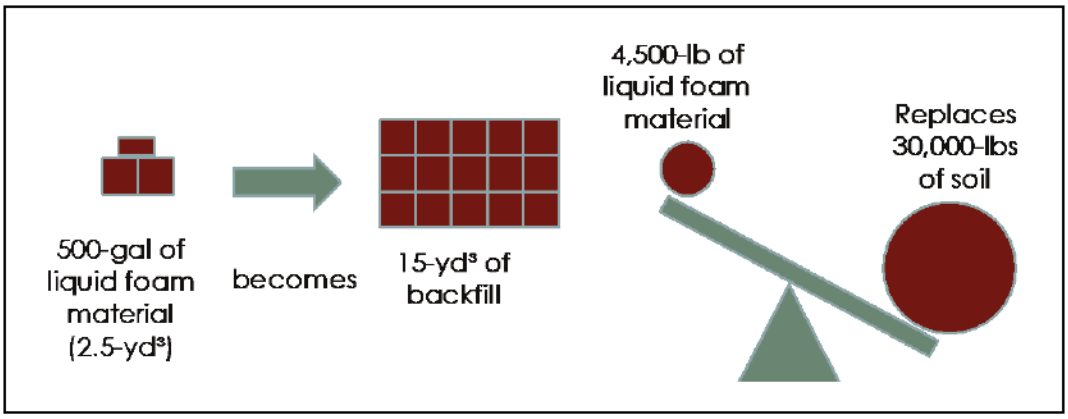

As noted, previous research conducted at the ERDC showed that polyurethane foam material is capable of providing sufficient compressive strength (200 psi) to support aircraft traffic under a concrete cap. The material has also been certified under live-flight testing (Priddy et al. 2013, Gurtowski et al. 2016).

2.7 Rapid-setting flowable fill

Rapid-setting flowable fill is a highly fluid mixture of rapid-setting cement, fly ash, fine aggregate, and water. Common applications of commercial flowable fill are for backfilling utility cuts and for use in pipe bedding. However, traditional commercial flowable fill products are not rapid setting. The rapid-setting material used in this experiment generally provides an UCS of 250 psi after 30 min of cure time and 750 psi after 3 hr of cure time. Post-trafficking investigations typically reveal a CBR of approximately 100% after 24 hr of cure time. It is packaged in 3,000-lb (1-yd³) super sacks and can be used as backfill material beneath rapid-setting concrete or asphalt.

2.8 Rapid-setting concrete

The surface material used in this experiment was CTS Rapid Set Concrete Mix®. It is a pre-blended, rapid-setting concrete material that has been identified by the ERDC as appropriate for crater capping due to its high early strength and load carrying capacity after only 2 hr of curing. The main cementitious component is Rapid Set Cement®, a proprietary material. Since the material is preblended and does not require the addition of local aggregates, it can be mixed in a variety of concrete mixing equipment when water is added. The aggregate in the mix is 3/8-in. maximum-size pea

gravel. Due to the fast set time of the material (10 to 20 min depending on temperature), bulk citric acid can be added to the mix water at elevated temperatures to increase the working time of the material and to prevent it from flash setting in the mixer. CTS Rapid Set Concrete Mix® achieves a UCS in excess of 3,000 psi after 2 hr and over 5,000 psi after 28 days. The material is packaged in 2,900-lb (0.93 yd^3) super sacks.

3 Experimental Program

3.1 Experiment layout

The experiment was conducted during the week of July 24-28, 2017, at the Outdoor Pavement Test Facility, on the East Campus of the Waterways Experiment Station, Vicksburg, MS. A total of eight (8) simulated craters were cut to 8.5-ft square and excavated to a depth of 34 in. (Figure 3.1). The simulated craters were arranged in two lanes of four (4) craters. Each lane represented a test sequence consisting of one repair per backfill method as shown in Figure 3.2. Figure 3.3 shows the repair profiles. An 11-in.-thick layer of compacted CL-ML was placed on top of the natural foundation at the bottom of the craters to provide a consistent subgrade throughout the craters. Some repairs were replicates, and others had specific variations between two sets of testing. For example, the chemical soil-stabilization backfill in Test Sequence 1 consisted of cement-stabilized silty sand (SM), while the repair in Test Sequence 2 was polymer-stabilized SM. The geocell backfill in Test Sequence 1 used sand (SP) while the geocell repair in Test Sequence 2 used SM. The foam and flowable fill backfills were intended to be replicates for both test sequences. However, some variations occurred during testing as discussed later in this report.

Figure 3.1. Simulated 8.5-ft square craters.

Figure 3.2. Repair layout for the test sequences.

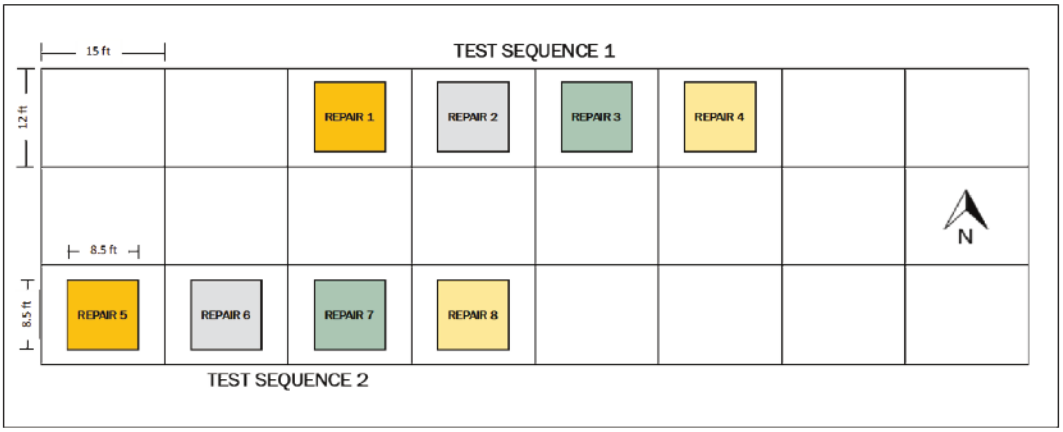

Figure 3.3. Repair profiles.

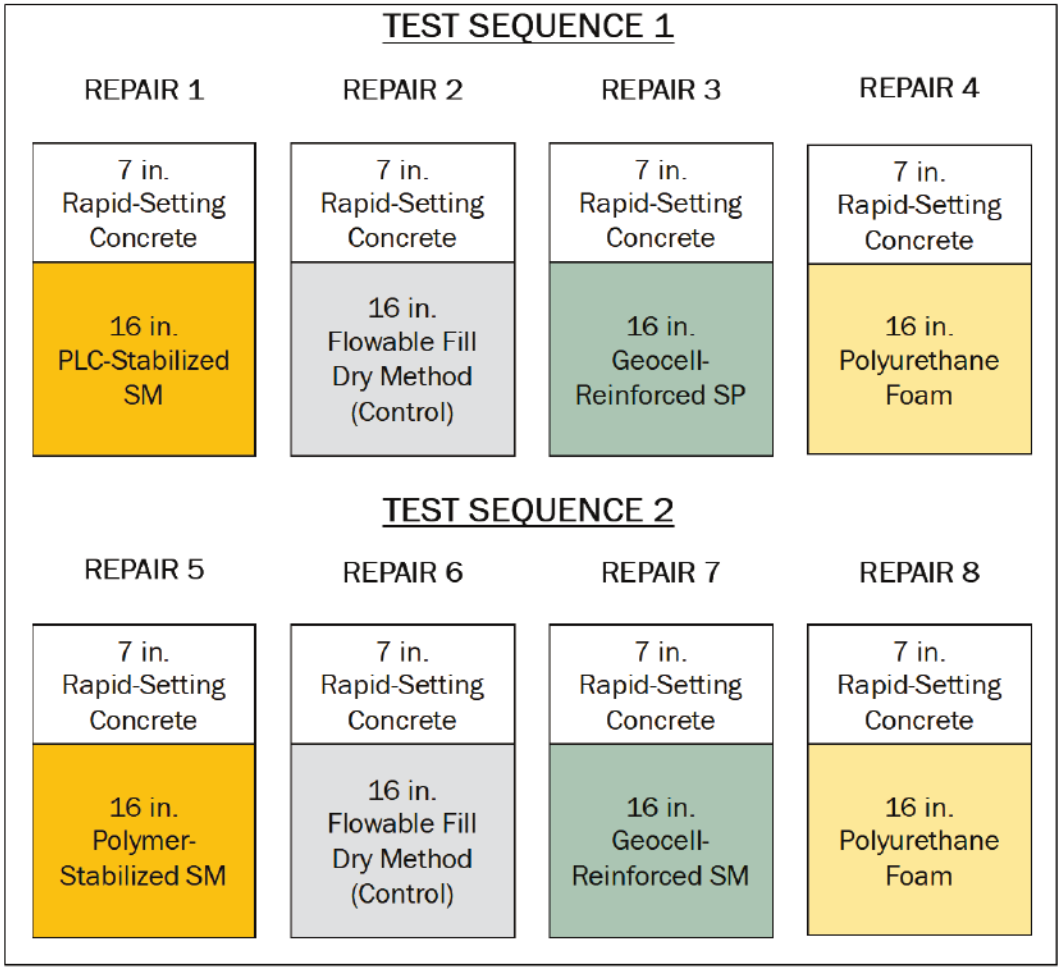

The target layer thicknesses for this experiment were 16 in. for the backfill and 7 in. for the rapid-setting concrete cap. These thicknesses deviated from

those established in the RADR TTPs (AFCEC 2018). The purpose of using 7 in. of rapid-setting concrete was to increase the impact of the backfill performance for each of the backfill technologies under a thinner cap. A thinner cap was expected to fail quicker and demonstrate the relative performance of the different backfill materials. ERDC already had data for some of the technologies under 6, 8, and 10 in. of rapid-setting concrete. The 16-in. backfill thickness was selected based on the required geocell heights in UFC 3-270-07, which states that two layers of 8-in. geocells were required underneath a thinner (7 in.) rapid-setting concrete cap. Therefore, a 16-in.-thick backfill was placed for all technologies to provide consistency between repairs. It important to note that this was done to allow meaningful comparisons between the backfills, and it was not intended to be used as recommendations for all backfill layer thicknesses.

The repairs were completed in three days with a team of seven (7) technicians, and the repair process consisted of only backfilling and capping the craters. Repairs 1 through 4 were completed on July 26. The backfills in Repairs 6 and 8 were completed on July 27, and the backfills in Repairs 5 and 7 were completed on July 28. The rapid-setting concrete caps in Repairs 5 through 8 were completed on July 28. The weather conditions during the experiment were generally hot and humid with cloudy skies. Table 3.1 provides a summary of weather conditions and repair tasks completed each day of the experiment.

Table 3.1. Weather conditions during the test period each day.

Date	Temperature Range (°F)	Relative Humidity Range (%)	Wind Speed (mph)	Repair Tasks Completed During Test period
July 26, 2017	76-92	50-97	0-5	Backfill Cap 2-hr traffic } Repairs 1 - 4
July 27, 2017	91-92	50-53	5-6	Backfill ⟶ Repairs 6 and 8
July 28, 2017	77-94	58-90	0-7	Backfill Repairs 5 and 7 Cap 2-hr traffic } Repairs 5 - 8

During each test sequence, the teams were divided into two teams of three (3) to work simultaneously on two backfill technologies. Once all four backfills were completed, the full team placed the rapid-setting concrete cap in all craters consecutively. Simulated F-15E aircraft traffic (112 passes) was applied to the four finished repairs 2 hr after the last repair cap was completed. Additional traffic was applied in the following days, as weather and scheduling allowed.

The following sections provide more details on the crater preparation, backfill construction, capping, and evaluation procedures.

3.2 Crater preparation

3.2.1 Construction of uniform subgrade

Each simulated crater was initially prepared by cutting the PCC surface with a 60-in. wheel saw attachment (Caterpillar SW60) on the Caterpillar compact track loader (CTL 279C), which was representative of cutting around upheaval for a crater repair. Once the repair was cut to size (approximately 8.5-ft square), the PCC was broken into smaller pieces with a moil-tipped hydraulic breaker (Bobcat HB1180) on a mini excavator (Bobcat E45 T4). Large debris and material underneath the PCC surface were then removed with the bucket attachment on the mini excavator. Each crater was excavated to a minimum depth of 34 in. to ensure that a uniform natural foundation (subgrade) was reached at the bottom of the crater repair. Dynamic cone penetrometer (DCP) (ASTM D6951 2018) data were collected on the subgrade and correlated to CBR strength values (Table 3.2). Photographs of this process are shown in Figure 3.4.

A silty clay (CL-ML) material was added in each simulated crater to provide a consistent and stable subgrade throughout the experiment. Each compacted CL-ML layer was at least 11-in. thick and was finished to a depth of 23 in. below the surface. The material was placed in approximately 3- to 4-in.-thick compacted lifts (5- to 6-in.-thick loose) to produce a uniform, constructed subgrade. Compaction of each lift was carried out by applying two coverages with a rammer, commonly called a jumping jack (Multiquip Mikasa MTX70 HD Rammer) compactor. A coverage consisted of starting compaction in one corner of the repair and working towards the center of the repair in a circular motion, and then returning in a circular motion towards the corner where compaction began. Photographs of subgrade construction are shown in Figure 3.5.

Figure 3.4. Cutting, breaking, and excavation process.

(a) Cutting PCC with wheel saw.

(b) Breaking PCC.

(c) Excavating to proper depth.

(d) Bottom of crater excavation.

Figure 3.5. Subgrade construction.

(a) Placing CL-ML lift into crater.

(b) Leveling CL-ML lift.

(c) Compacting CL-ML lift with jumping jack.

Nuclear moisture and density measurements (ASTM D6938 2017b) and DCP tests (ASTM D6951 2018) were conducted to verify the stiffness of the natural foundation (natural soil) and constructed subgrade layers and to ensure they were consistent throughout all the craters. Data are shown in Tables 3.2 and 3.3. Natural foundation CBR values ranged from 5 to 11%. The compacted subgrade CBR values ranged from 19 to 27%.

Table 3.2. Crater natural foundation and compacted subgrade DCP tests results.

Crater No.	Test Location	Average CBR (%)			
		Natural Foundation		Compacted Subgrade	
1	NW	4	**5**	19	**19**
	C	6		19	
	SE	5		18	
2	NW	6	**6**	18	**19**
	C	6		21	
	SE	5		19	
3	NW	5	**5**	28	**19**
	C	5		18	
	SE	6		13	
4	NW	4	**4**	30	**26**
	C	5		26	
	SE	4		22	
5	NW	5	**8**	19	**19**
	C	9		19	
	SE	9		19	
6	NW	12	**11**	26	**25**
	C	8		19	
	SE	12		30	
7	NW	9	**10**	26	**27**
	C	12		25	
	SE	9		30	
8	NW	7	**10**	26	**26**
	C	9		32	
	SE	15		24	

Table 3.3. CL-ML constructed subgrade average nuclear moisture and density.

Crater No.	1	2	3	4	5	6	7	8
Dry Density, pcf	98.2	99.7	95.7	100.6	100.1	101.1	102.3	100.0
Wet Density, pcf	111.2	112.0	91.2	115.7	113.8	114.1	117.0	114.0
Moisture, %	13.2	12.6	12.7	15.2	13.7	13.5	14.4	14.1

The surface of the constructed subgrade was surveyed with a rod and level to later verify the thickness of the backfill. Data were collected as shown in Figure 3.6, which is the recommended method reported by Priddy et al. (2016). Survey points were located along three lines

(labeled N, C, and S representing North, Center, and South, respectively) in the direction of traffic. Survey points were also collected for the cross section, labeled CS in Figure 3.6.

Figure 3.6. Location of survey points.

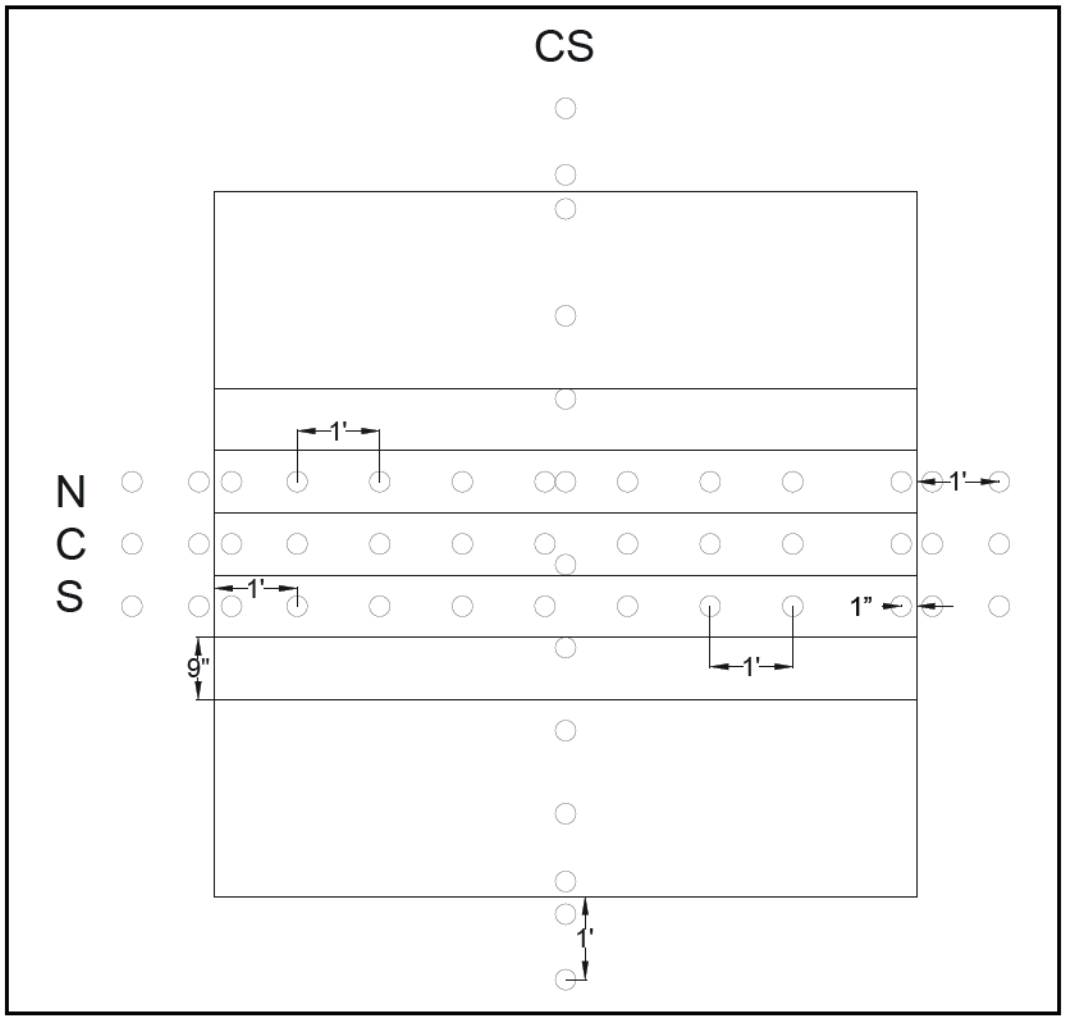

3.2.2 Instrumentation (EPCs)

One earth pressure cell (EPC) was installed on the surface of the constructed subgrade in each repair to measure the magnitude and changes in pressure below the backfill material during traffic. The EPCs were installed at the center of each crater, as shown in Figure 3.7, and were connected to a data acquisition box that was placed nearby to the craters. During each test sequence, data were continuously recorded while simulated traffic was being applied to the repairs.

Figure 3.7. EPC being installed at the center of a repair over the constructed subgrade.

3.3 Backfill construction

3.3.1 Chemically stabilized soil backfill (Repairs 1 and 5)

Chemically stabilizing soil with either polymer or cement was used to potentially increase the strength of low quality backfill with minimal equipment and materials. The ability to use locally available soil decreases the logistical footprint in terms of material required. A polymer, Soil-Sement®, and PLC were chosen to be the additives for the two chemically stabilized soil backfill crater repairs. A blended SM was used as the soil for the chemical-stabilized backfill, and both the polymer and PLC additives were placed using a similar methodology.

The mixing process required a team of three (3) people. To ensure the correct amount of soil was mixed, the soil was carefully laid out in a 21-ft by 10-ft blend area, at a height of 1 ft with the front-end loader (Figure 3.8). The SM was at a moisture content of approximately 8.2%, which was slightly above the optimum moisture content of 7.9% (Appendix C). According to ETL 12-7 (AFCEC 2012), it is recommended to use 1% more moisture content than the optimum moisture content. However, based on

previous laboratory testing, 5% PLC at an 8% moisture content was recommended for field testing (Johnson et al. 2018). To achieve the 5% PLC, 3.34 lb of PLC was added per cubic foot of loose soil. A total of 700 lb of PLC was added to the soil for this testing. The PLC was packaged in 50-lb buckets, and half of the total PLC, seven buckets, were incorporated at a time, as shown in Figure 3.9.

Figure 3.8. Placement of soil in 21-ft by 10-ft area.

Figure 3.9. Addition of PLC.

To blend the PLC and soil, a tiller attachment (Caterpillar LT13B) on the CTL was utilized (Figure 3.10). Once the CTL with the tiller attachment mixed the soil with half of the required cement, the front-end loader bucket was used to flip the soil to ensure homogeneity. The remaining half of the cement was distributed evenly on the soil, and the CTL with the tiller attachment resumed mixing the soil. After mixing, the front-end loader was once again utilized to flip the stockpile.

Figure 3.10. CTL tiller attachment (Caterpillar LT13B) used to blend soil with additive.

To blend the soil with the Soil-Sement® polymer emulsion, a 1/6-hp submersible utility pump was placed into the polymer drum, and a hose was used to distribute the product (Figure 3.11). The polymer was added at a rate of 3% by weight of soil -- approximately 0.225 gal of polymer per cubic foot of loose soil. The SM soil moisture content was approximately 7.5%, which was just under the optimum moisture content of 7.9%. It was important to make sure that the soil is at or below optimum because the polymer emulsion would add moisture to the mixture. To mix the polymer emulsion, the loose soil was laid out similar to the cement-mixing method in a 21-ft-long by 10-ft-wide area at a height of 1 ft. For this test, a total of 47 gal of Soil-Sement® polymer emulsion was used. Initially, approximately 27 gal was sprayed using the submersible utility pump and hose (Figure 3.12). The CTL with tiller attachment mixed the soil, and the

front-end loader was used to flip the soil. This process was repeated with the remaining 20 gal of polymer emulsion.

Figure 3.11. Submersible utility pump in 55-gal drum of polymer.

Figure 3.12. Spraying polymer emulsion on loose soil.

For both PLC and polymer mixed soil, the backfill placement process was executed by placing the mixed soil in four 4-in.-thick compacted lifts to obtain a total compacted thickness of 16 in. The mixed soil was placed by a team of three (3) people using a front-end loader and shovels. For each lift, the stabilized soil was placed into the crater above the desired level to account for compaction and was compacted with two coverages of a jumping jack (Multiquip Mikasa MTX70 HD rammer) (Figure 3.13). A coverage is defined as starting compaction in one corner, working in a spiral pattern towards the center, and spiraling back around to the starting point. The final top surface was compacted with a plate compactor (Northern Industrial JPC-80) for two additional coverages to ensure a flat surface was achieved (Figure 3.14). The plate compactor was not a required step but, since this was a controlled test, more attention was focused on the final surface of the backfill to ensure thickness consistency between repairs.

The cement-stabilized soil was placed in the morning and was capped later that afternoon, giving it approximately 4 hr to cure. This cure time was a result of the test sequence and not considered a requirement. The polymer-stabilized soil was placed on one day and that repair was not capped until the following day. In this case, the curing time was approximately 24 hr, but also a result of logistical planning and not a requirement.

Figure 3.13. Compacting soil.

3.3.2 Rapid-setting flowable fill backfill (Repairs 2 and 6)

Approximately 3.5 super sacks of dry material were used to complete 16 in. of rapid-setting flowable fill backfill in the 8.5-ft × 8.5-ft repairs. The material was placed in 6-in. lifts. Each lift consisted of placing one super sack of dry material in the excavated repair, and then applying approximately 40 to 50 gal of water to the surface. The water was allowed to percolate through the dry material by gravity before placing the next lift. Figure 3.15 shows flowable fill being placed inside Repair 2 using the dry placement method. Figure 3.16 shows the process of adding water to the rapid-setting flowable fill. The finished rapid-setting flowable fill surface is shown in Figure 3.17. Equipment required for rapid-setting flowable fill placement included one telehandler for transporting the super sacks of rapid-setting flowable fill from the staging area to the excavated hole, a water truck with a water flow meter, and assorted hand tools such as rakes and shovels to distribute the dry material in the repair.

Figure 3.14. Final surface preparation with plate compactor.

Figure 3.15. Rapid-setting flowable fill dry placement method.

Figure 3.16. Adding water to rapid-setting flowable fill during dry placement method.

Figure 3.17. Finished rapid-setting flowable fill surface.

3.3.3 Geocell-reinforced backfill (Repairs 3 and 7)

Once the constructed subgrade was compacted for Repairs 3 and 7, the horizontal dimensions of the crater were measured so that the geocell sections and geotxtile could be cut to size (Figure 3.18). Tools for cutting the geocell sections and geotextile to the appropriate size included utility knives, a measuring tape, rebar, and hammers.

Figure 3.18. Cutting geocell section to fit crater size.

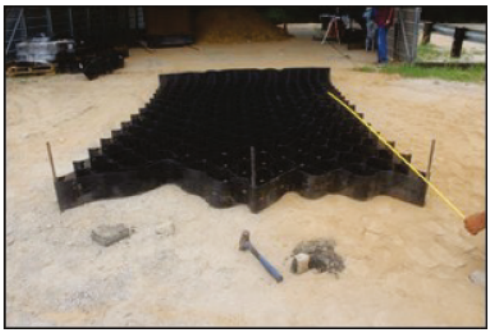

(a) Measuring geocell section.

(b) Cutting geocell section with utility knife.

Once geocell sections were cut, the installation of the geocell-reinforced backfill for each repair was as follows (Figure 3.19).

1. The bottom of the excavation was lined with the nonwoven, 6-oz, needle-punched, polypropylene geotextile.
2. The first layer of geocells was expanded parallel to the centerline. Rebar was placed at all corners of the repair to hold the expanded

geocell section in place. Backfill material was used to fill some of the geocell pockets along the edges to help hold the geocell section in place.

3. The geocell section was backfilled using a CTL with a bucket attachment to drop the material vertically into the repair to avoid displacing the geocell section. The geocell section was overfilled by approximately 2 in., and the material was spread evenly with shovels and rakes.
4. The SP backfill in Repair 3 was compacted using the Northern Industrial JPC-80 plate compactor until the sand appeared to be nearly level with the geocell section. The SM backfill in Repair 7 was compacted using the Multiquip Mikasa MTX70 HD Rammer, or jumping jack. Any excess material was struck level with the top of the geocell using shovels and rakes.

Figure 3.19. Geocell-reinforced backfill placement.

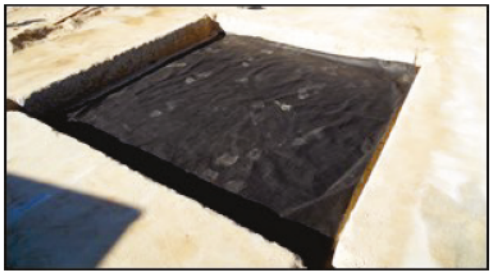

(a) Fabric placed over the constructed subgrade.

(b) Geocell section placed in crater

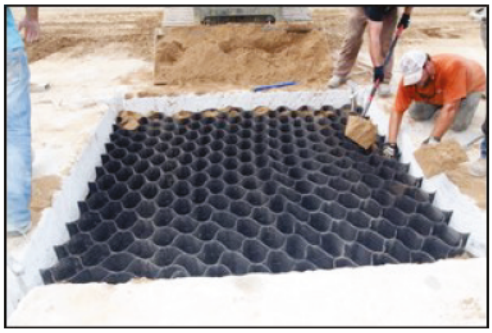

(c) Placing SM along edges (Repair 7).

(d) Backfilling geocells with SM (Repair 7).

(e) Spreading SP evenly with rakes (Repair 3).

(f) Compacting SP with plate compactor (Repair 3).

5. The surface of the first layer of geocells was then lined with the non-woven, 6-oz, needle-punched polypropylene geotextile.
6. The second layer of geocells was expanded perpendicular to the center-line and held in place, as described in Step 2.
7. The second layer of geocells was backfilled and compacted, and excess material was removed, as described in Steps 3 and 4.

Data collection on each layer of geocell-reinforced soil was subjected to nuclear moisture and density and DCP test. The surface was also surveyed with a rod and level to determine the thickness of the geocell-reinforced base. The target thickness was 16 in. (two 8-in.-thick layers of geocells). Each repair was capped with Rapid-Set Concrete as described later in this chapter.

3.3.4 Foam backfill (Repairs 4 and 8)

The foam backfill was placed using a prototype automated foam distribution system (Figure 3.20), to dispense liquid foam material into the excavated repair and then allowing the foam to expand and set before the rapid-setting concrete cap was applied.

Figure 3.20. CRADR 1-L prototype foam dispensing system.

The foam backfill process was as follows.

1. The excavated repair dimensions were measured and entered into the automated foam distribution system through the touch screen control

panel. The required measurements, in inches, were the total width, length, and depth of the repair, as well as the desired cap thickness.

2. The bottom of the excavation was lined with 10-mil polyethylene plastic sheeting, making sure that the liner was in contact with the excavation walls and corners. Rebar was installed to hold the liner in place (Figure 3.21).
3. The foam dispenser (Figure 3.22) was operated by following the procedures indicated in the user's manual. All of the fluid lines and the mixing head were connected in advance to save time during the repair process. Crater dimensions varied slightly between Repair 4 and Repair 8, thus requiring different foam pour times for each crater (Figure 3.23 and Figure 3.24). The liquid polyurethane foam mix was dispensed in approximately 4 to 6 min. Once the liquid foam placement was completed, the mixing head was disconnected from the fluid lines and placed in a bucket for draining.

Figure 3.21. Polyethylene liner applied to Repair 4.

Figure 3.22. Foam placement.

Figure 3.23. Placing additional foam in Repair 4 to achieve the desired backfill thickness.

Figure 3.24. Final foam backfill surface of Repair 4.

4. The foam was allowed to expand and cure for about 10 min. At that point, the excess liner was cut and removed. When the foam expanded in each excavated repair, an uneven and cracked domed surface was formed (Figure 3.25). Therefore, the foam surface was inspected to identify areas that required leveling or cutting so that a smooth and level surface was provided for the required 7-in. cap thickness. These domed areas were cut with a reciprocating saw, and the excess material was discarded.
    a. On Repair 4, the dispensed foam liquid was not enough to produce a 16-in.-thick layer. Therefore, an additional layer of foam was poured on top. Since the foam surface on the first layer was uneven, the liquid foam was deposited in the low areas creating more of an uneven overall surface. The second layer foam was soft to the touch and did not bond very well to the first layer. No cutting was required on Repair 4.
    b. On Repair 8, the foam was dispensed in a single pour. However, the expanded foam surface was very uneven and cracked. Cutting was required to meet the thickness requirement (Figure 3.26).
    c. The target backfill thickness was 16 in. However, since the expanded foam backfill surfaces were uneven, the backfill thicknesses varied throughout the repairs. The average foam layer thicknesses were 14 in. and 15 in. in Repair 4 and Repair 8, respectively.

Figure 3.25. Expanded foam backfill surface of Repair 8.

Figure 3.26. Final foam backfill surface of Repair 8 (after cutting).

3.4 Repair backfill assessment using light weight deflectometers

After each backfill was completed for each repair, two lightweight deflectometers (LWDs) were used to quantify the relative backfill stiffness by measuring the deflections resulting from a known force. This method consisted of dropping a mass to incur a dynamic load to a plate on the ground, and a buffer was used to simulate vehicle traffic by modifying the impact of the load. The maximum deflection along with the peak force was used to estimate the dynamic modulus, as shown in Equation 1, where A is the stress distribution factor, υ is the soil Poisson's ratio, w_o is the peak

vertical deflection, F_{pk} is the peak applied load, and r_o is the radius of the load plate (Stamp and Mooney 2013).

$$E_{LWD} = \frac{A(1-v^2)F_{pk}}{\pi r_o w_o} \quad (1)$$

Although the two LWD devices measure the vertical deflection differently, Equation 1 was utilized to provide an estimated dynamic modulus for both. Data were collected on all of the crater repairs, with the exception of the foam backfill repairs. The foam backfill returned an error on both devices, possibly because of the uneven surface.

The Dynatest LWD Model 3031 (Figure 3.27) follows ASTM E2583-07 (ASTM 2015a) and ASTM E2835-11 (ASTM 2015b). To operate the device, a 10-kg load was dropped from a maximum height of 850 mm onto a 300-mm-diam plate with a rubber buffer. The load cell measured the applied load and peak magnitude, while a geophone measured the deflection in the center of the device. To run the Dynatest LWD, the load was dropped three times to seat the device, and the subsequent two readings were recorded. The LWDmod software was used to determine the modulus, E, and is reported in Table 3.4 along with the maximum deflection, s.

The Zorn ZFG 3000 GPS (Figure 3.28) follows ASTM E2835-11 and has a 10-kg load that is dropped onto a 200-mm-diam, 40-mm-thick plate to estimate the dynamic deflection modulus using the measured deflection, s (mm). The maximum pulse force is 7.07 kN, and the pulse duration is 17 ms. To run the Zorn LWD, three seating drops were completed to seat the device, and the readings from following three drops were averaged by the device to provide the deflection and dynamic deflection modulus for the test location. The ZFG 3000 software was used to determine the modulus, E, and is reported in Table 3.4 along with the maximum deflection, s.

Figure 3.27. Dynatest LWD Model 3031.

Table 3.4. Backfill LWD deflection and modulus results.

Repair No.	Backfill Technology	Test Location	Dynatest				Zorn			
			s[a] (mm)	Average s[a] (mm)	E (MPa)	Avg E (MPa)	s[a] (mm)	Average s[a] (mm)	E (MPa)	Avg (MPa)
1	Cement-Stabilized SM	NW	0.056	0.047	947	1078	0.189	0.194	159	154
		C	0.038		1208		0.202		149	
		SE	—[b]		—[b]		0.192		156	
2	Rapid-Setting Flowable Fill	NW	—[b]	0.074	—[b]	1413	0.092	0.076	326	403
		C	0.039		2082		0.070		429	
		SE	0.108		744		0.066		455	
3	Geocell-Stabilized SP	NW	3.271	1.801	20	49	4.148	4.507	7	7
		C	0.888		75		4.980		6	
		SE	1.244		52		4.394		7	
5	Polymer-Stabilized SM	NW	0.403	0.471	59	52	1.085	1.048	28	29
		C	0.512		43		1.072		28	
		SE	0.497		53		0.988		30	
6	Rpaid-Setting Flowable Fill	NW	0.049	0.036	531	758	0.071	0.080	423	402
		C	0.027		896		0.109		275	
		SE	0.032		848		0.059		508	
7	Geocell-Stabilized SM	NW	1.060	0.911	21	28	3.897	2.694	8	12
		C	0.709		37		2.086		14	
		SE	0.965		26		2.098		14	

[a] Measured maximum deflection.

[b] Unavailable data.

[c] No data were recorded for the foam backfilled craters of Repairs 4 and 8.

Figure 3.28. Zorn ZFG 3000 GPS.

Results from both devices indicated that cementitious-type backfills, the rapid-setting flowable fill and cement-stabilized backfills, were the stiffest. The Zorn LWD showed that both of the rapid-setting flowable fill repairs (2 and 6) were the strongest, with similar modulus values of 402 and 403 MPa and small deflection values of 0.080 and 0.076 mm. The Dyna-test LWD showed that the stabilized cement and flowable fill have small deflection values of 0.074 mm or less, and modulus values greater than 758 MPa. The remaining backfill repairs with the polymer-stabilizer and the geocells had much lower values than the rapid-setting flowable fill and cement-stabilized backfills. The polymer-stabilized backfill showed approximately double the modulus values than the geocell backfill, but the polymer backfill was much less stiff than the cementitious-type backfill. The polymer backfill required more curing time, and for water to evaporate and increase strength in the polymer-stabilized backfill.

3.5 Rapid-setting concrete cap placement

The rapid-setting concrete cap was placed by a team of seven (7) people including a mixer operator, a forklift operator, two screed operators, and three hand-tool workers. The volumetric mixer (Figure 3.29) was filled with approximately six super sacks of Rapid Set Concrete Mix® prior to the starting the pour. However, a forklift was required to consistently

feed the mixer with Rapid Set Concrete Mix® material to keep enough material weight on the dry material belt to get a consistent mix. The mix was poured into each crater until reaching the surface level. Concrete rakes were used to distribute the mix throughout the crater. The screeding process was performed by hand using a straight-edge bar (Figure 3.30). Concrete hand-finishing was performed after screeding by using aluminum or magnesium trowels. Once all repairs in a test sequence were capped, the mixer was pressure-washed to remove residual material. No intermediate wash was required between crater repairs. Figures 3.31 through 3.38 show the finished rapid-setting concrete surfaces for all eight repairs before traffic was applied.

Figure 3.29. Volumetric mixer.

After trafficking, core samples were collected from three different locations in each repair to determine the rapid-setting concrete unconfined compressive strength (UCS) and to verify the cap thicknesses. The core samples were collected 56 days after construction.

Figure 3.30. Rapid-setting concrete cap screeding with straight-edge bar.

Figure 3.31. Finished rapid-setting concrete cap on Repair 1.

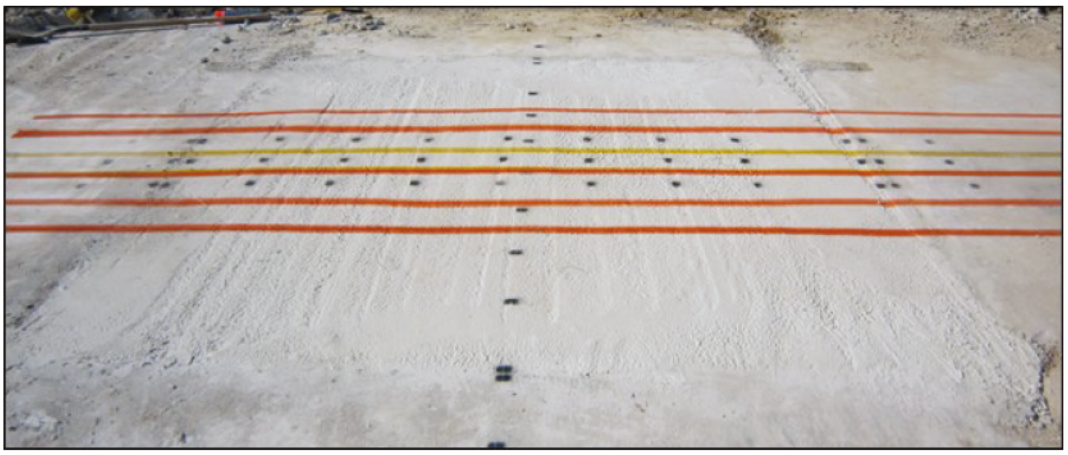

Figure 3.32. Finished rapid-setting concrete cap on Repair 2.

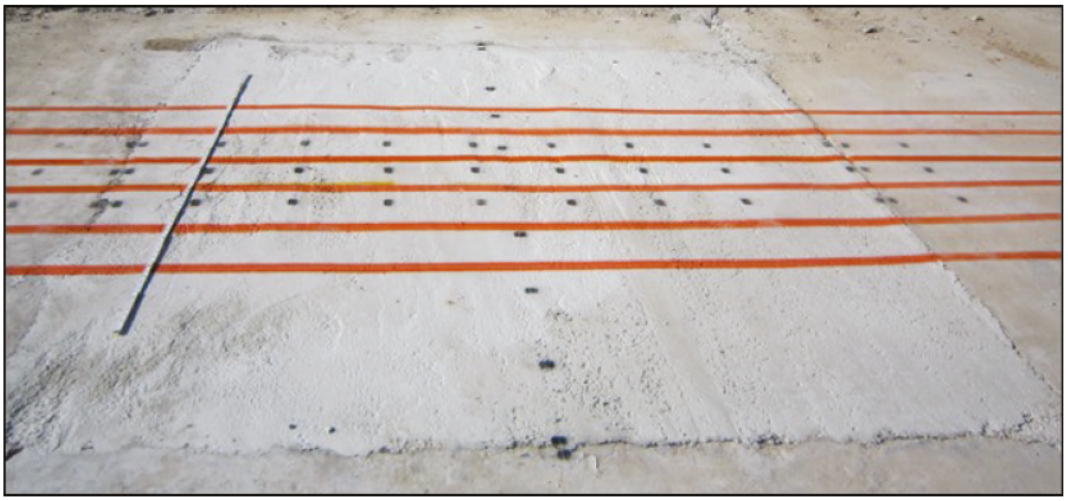

Figure 3.33. Finished rapid-setting concrete cap on Repair 3.

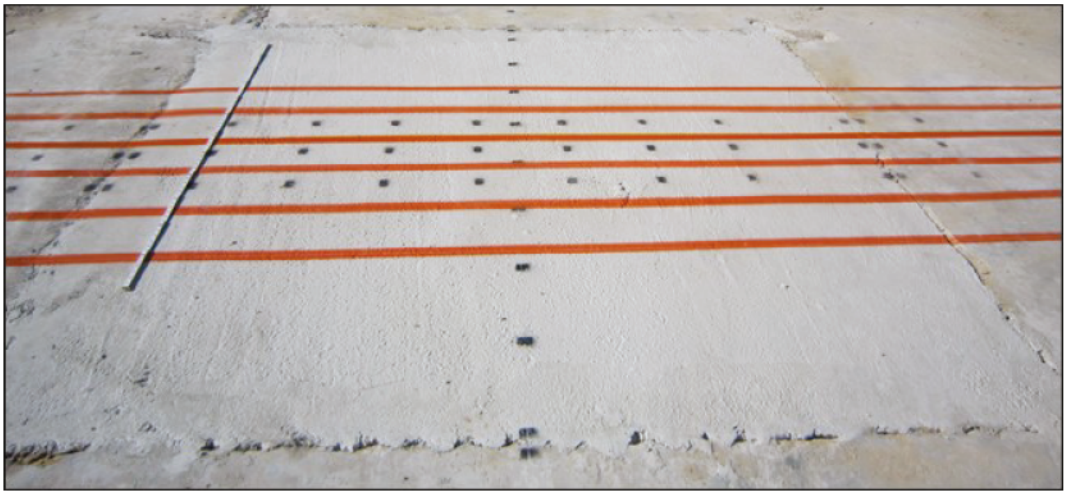

Figure 3.34. Finished rapid-setting concrete cap on Repair 4.

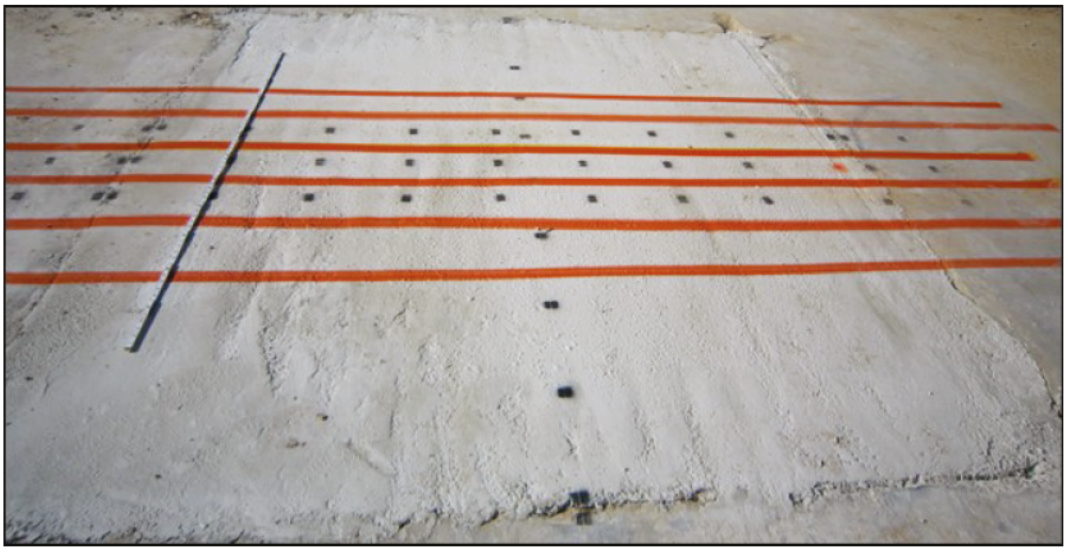

Figure 3.35. Finished rapid-setting concrete cap on Repair 5.

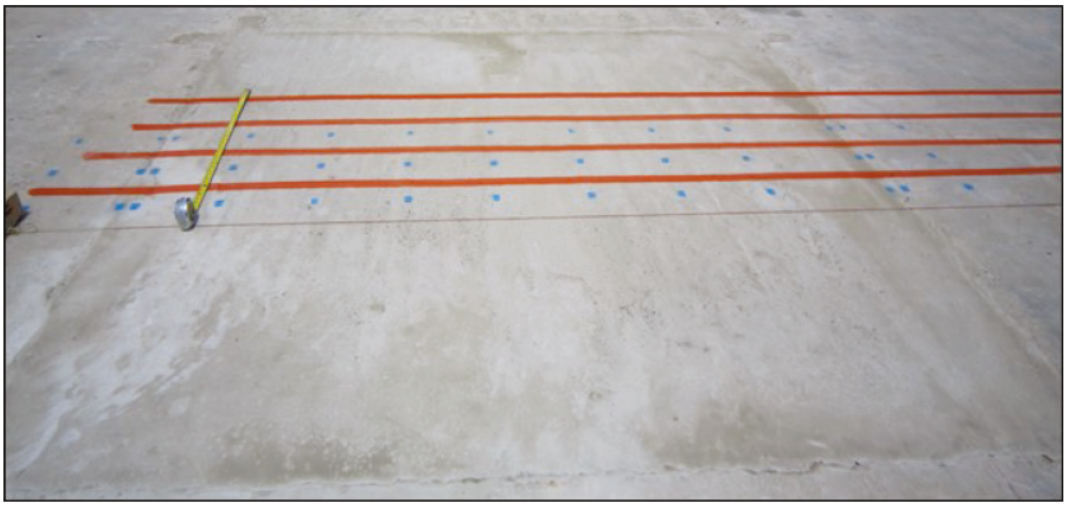

Figure 3.36. Finished rapid-setting concrete cap on Repair 6.

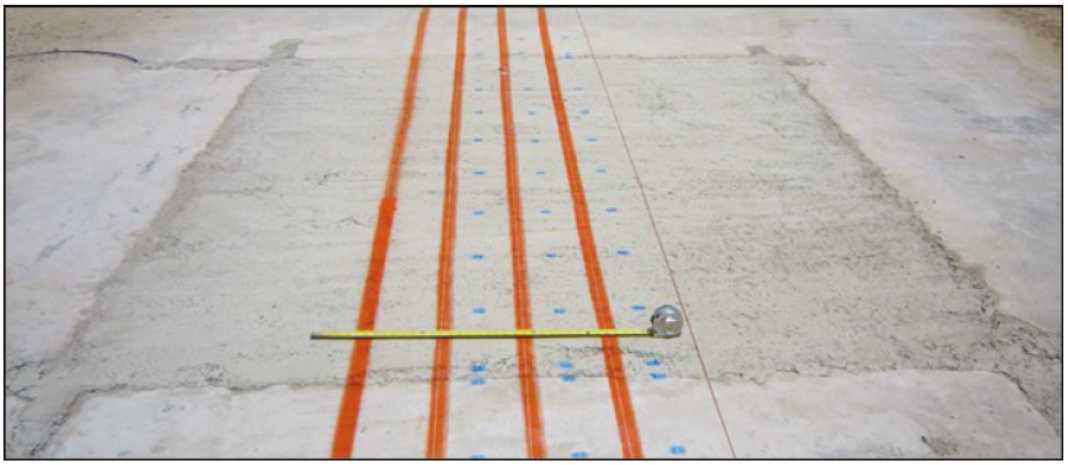

Figure 3.37. Finished rapid-setting concrete cap on Repair 7.

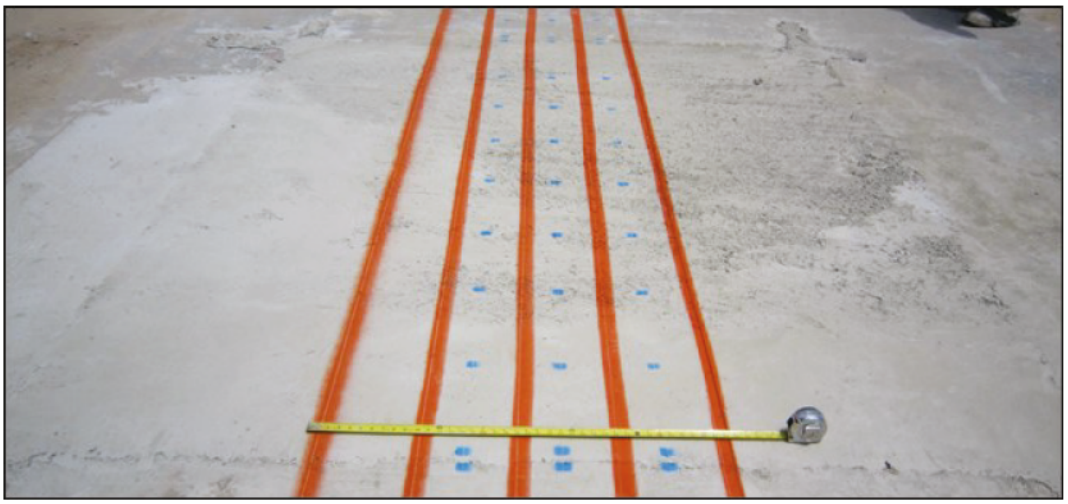

Figure 3.38. Finished rapid-setting concrete cap on Repair 8.

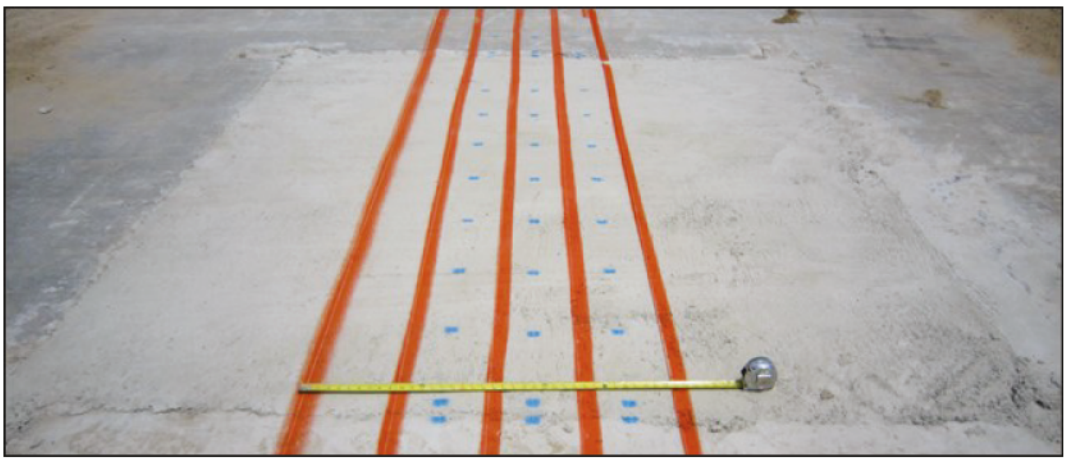

3.6 Simulated aircraft traffic operations

Simulated aircraft traffic was applied to the repairs 2 hr after the rapid-setting concrete caps were completed. A single-wheel F-15E load cart (Figure 3.39) equipped with a 36-in.-diam, 11-in.-wide, 18-ply tire inflated at 325 psi was used. The gross wheel load was approximately 35,235 lb. A normally distributed pattern of simulated traffic was applied in a 3.75-ft-wide traffic lane as shown in Figure 3.39. Traffic was applied by driving the load cart forward and then backward in the same wheel path, then moving laterally approximately one tire width (9 in.) on each forward pass. A total of 16 passes constituted one traffic pattern. After the first 112 passes were completed and data were collected, the repairs were trafficked until failure or until 3,600 passes. Failure of the repairs was defined as a high-severity shattered slab or spalls that were 2 in. deep. If at any point during trafficking high FOD potential or tire hazards were identified in a given repair, it was considered failed, and traffic was discontinued on that repair.

Figure 3.39. F-15E load cart and typical F-15 normally distributed traffic pattern.

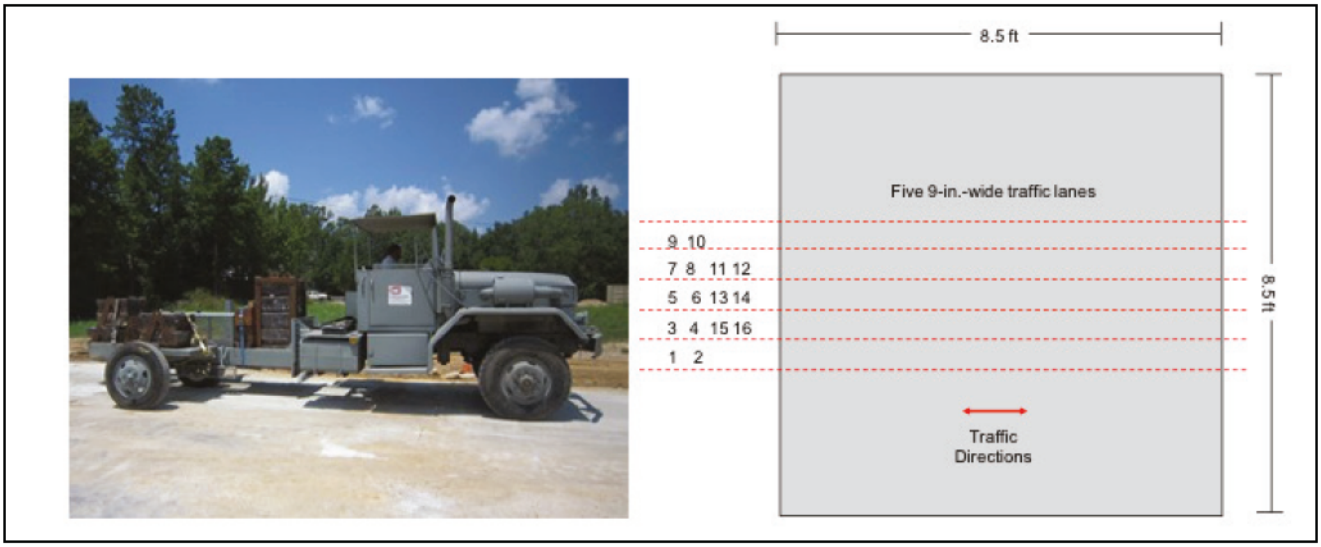

3.7 Data collection

Prior to trafficking, the surface of each repair was inspected for any pre-traffic distresses. After 112 passes, the surface of each repair was inspected again. The repairs were then inspected at 200- to 500-pass intervals until they failed, or until 3,600 passes were completed. Cracks were measured and marked using paint sticks, and photographs were taken to document

the crack/failure progression. Spalling was measured for length, width, and depth (Figure 3.40). Loose, spalled material was also measured, and the average size of particles was recorded.

Each repair was also surveyed using a rod and level prior to trafficking, at 112 passes, and at failure or 3,600 passes. The survey data were used to measure any permanent deformation that occurred and to determine elevation changes at the joint due to removal of spalled material during trafficking. Data were collected as shown in Figure 3.6, with survey points along three lines in the direction of traffic and along the cross section (Figure 3.41).

Figure 3.40. Measuring a spall on repair edge.

A Falling Weight Deflectometer (FWD) was employed in the center of each repair and on a control slab within the test site in order to monitor changes in stiffness of Repairs 1-7 (Figure 3.42). FWD data were not collected on the foam-backfilled repairs 4 and 8. The control slab was not trafficked. FWD data were collected prior to trafficking, after 112 passes, and then at 200- to 500-pass intervals until failure, or when 3,600 passes were completed.

Figure 3.41. Survey data collection.

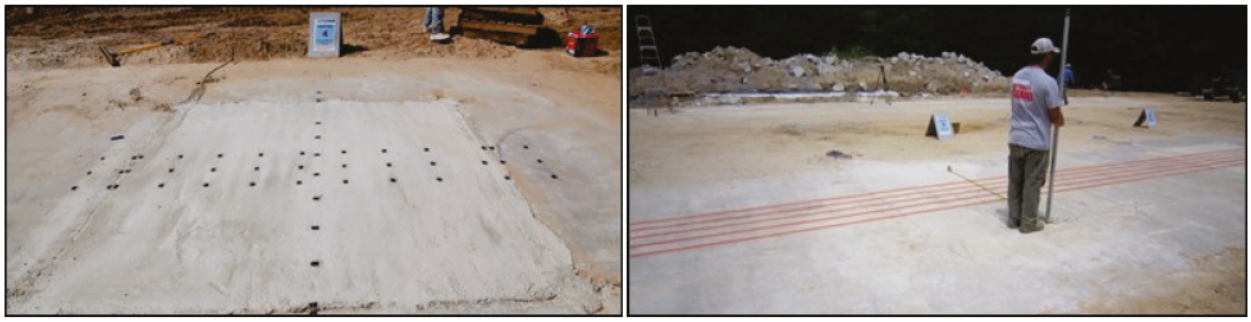

(a) Points on repair surface.

(b) Rod and level data collection.

Figure 3.42. FWD testing on the surface of a repair.

4 Results

4.1 Repair data summary

Table 4.1 provides a summary of the finished repair layer thicknesses and strength properties. All repairs met the required thicknesses, except for the foam backfill repairs (4 and 8). As was discussed previously, the foam surfaces were uneven with overall thicker center areas and thinner edges. This caused the average thicknesses to be a little lower than required, consequentially causing the rapid-setting concrete cap to be thicker around the repair edges. Most rapid-setting concrete cap thicknesses determined by measuring extracted core samples match the thicknesses calculated from the survey data, except for Repair 4. For this repair, two of the three core samples were extracted near the edges where the rapid-setting concrete was thicker. The thickness from the survey data was calculated by averaging the measurements throughout three profiles and one cross section of the repair.

Table 4.1. Repair data summary.

Repair No.	Backfill Technology	Backfill Properties				Rapid-Setting Concrete Cap Properties		
		Thickness (in.)	CBR from DCP (%)	Dry Density (pcf)	Moisture Content (%)	Average Thickness from Survey Data (in.)	Average Thickness From Cores (in.)	Unconfined Compressive Strength[a] (psi)
1	Cement-Stabilized SM	15.7	95	124.3	6.8	7.0	7.0	4,653
2	Rapid-Setting Flowable Fill	15.9	100	N/A	N/A	6.9	7.0	9,867
3	Geocell with SP	16.0	7	101.1	7.6	6.7	7.1	9,660
4	Foam	13.9	N/A	N/A	N/A	8.9	10.5	9,847
5	Polymer-Stabilized SM	16.0	18	122.4	8.6	6.9	6.6	10,353
6	Rapid-Setting Flowable Fill	15.0	100	N/A	N/A	7.0	7.0	9,560
7	Geocell with SM	15.3	32	115.7	8.4	7.4	7.5	8,610
8	Foam	15.4	N/A	N/A	N/A	8.2	7.9	9,353

[a] Tested 56 days after construction.

When performed, DCP tests in the rapid-setting flowable fill backfills resulted in refusals, i.e., penetration was less than 0.08 in. after five (5) blows or the rod was deflected more than 3 in. from the vertical position due to the presence of aggregates. Therefore, the rapid-setting flowable fill was considered 100-CBR material. DCP test data showed that the cement-stabilized SM was the second strongest backfill after the flowable fill. The data also indicate that SM soil stabilization using

cement produced a better quality backfill than when polymer or geocells were used to stabilize the SM soil. DCP testing may not be indicative of the bearing capacity of geocell confined materials due to the nature of the reinforcement and the small diameter cone.

DCP testing was not conducted on the foam backfills (Repairs 4 and 8) during this experiment. However, DCP data from a subsequent field experiment using foam backfill in similar repair conditions showed DCP penetration rates in the foam backfill of 20 to 25 mm/blows, which is typical of soils with CBR values ranging from 8 to 10% (Bell et al. 2019).

UCS testing results of core samples obtained from the rapid-setting concrete cap showed that all caps had appropriate strength. However, in Repair 1, the UCS after 56 days was 4,653 psi, which was a lot lower than expected. Typically, CTS Rapid Set Concrete Mix® produces UCS values of over 8,000 psi after 28 days.

4.2 Backfill placement times

The backfill placement times are shown in Figure 4.1. The TTPs established a threshold time of 11 min for placing 14 in. of flowable fill using the dry method in 8.5-ft crater repairs. However, the backfills placed during this experiment were 16 in. thick. It is important to note that in this experiment, the repairs were conducted by a crew of engineering technicians under experimental conditions and not during a simulated operational scenario with a sequential repair process. Therefore, these times will be used in this report only for comparing between backfill technologies.

The standard backfill method for dry placement of rapid-setting flowable fill was completed in 20 min in Repair 2 and 22 min in Repair 6. The methods that took the longest time to complete were the chemical soil-stabilization backfills, which were completed in 75 min and 90 min in Repairs 1 and 5, respectively. These methods involved laying out soil, adding the chemicals (cement or polymer), mixing the chemicals with the soil using a tiller, flipping the soil to complete the mixing process, placing the soil in the crater in layers, and applying compaction. This process was very time-consuming and labor-intensive. The geocell backfill method required less time than the chemical-stabilized soil backfill (43 and 66 min). However, the process of installing the geocells, dumping the soil in the geocell pockets, compacting, and then repeating these steps for the

second layer was still more time-consuming and labor-intensive than the standard rapid-setting flowable fill backfill method.

The fastest method of backfill placement was the foam backfill. In both Repair 4 and Repair 8, it took less than 15 min to complete the foam backfill process of setting up the dispensing equipment, measuring the crater dimensions, installing the plastic liner, and dispensing the liquid foam into the crater. After the foam expanded, the excess liner was cut, and the crew was ready to move forward to the next task. As discussed in Section 3.3.4 on Repair 8, the foam surface was uneven and required cutting. This task added 25 min to the process. However, cutting was performed by the project engineers while trying different cutting techniques. Therefore, this time was not considered realistic. Previous experiments during simulated operational scenarios (Bell et al. 2019, Mejias-Santiago et al. draft*) have shown that cutting could take from 5 to 10 min. if only the high spots on the foam backfill are cut down to ensure an even rapid-setting concrete cap thickness (10 in. minimum).

* Mejias-Santiago, M., J. S. Tingle, J. L. Johnson, L. A. Gurtowski and C. S. Griggs. Draft. *Refinement of foam backfill technology for expedient airfield damage recovery Phase III: Technology demonstration and end user evaluation*. ERDC/GSL TR. Vicksburg, MS: U.S. Army Engineer Research and Development Center.

Figure 4.1. Backfill times.

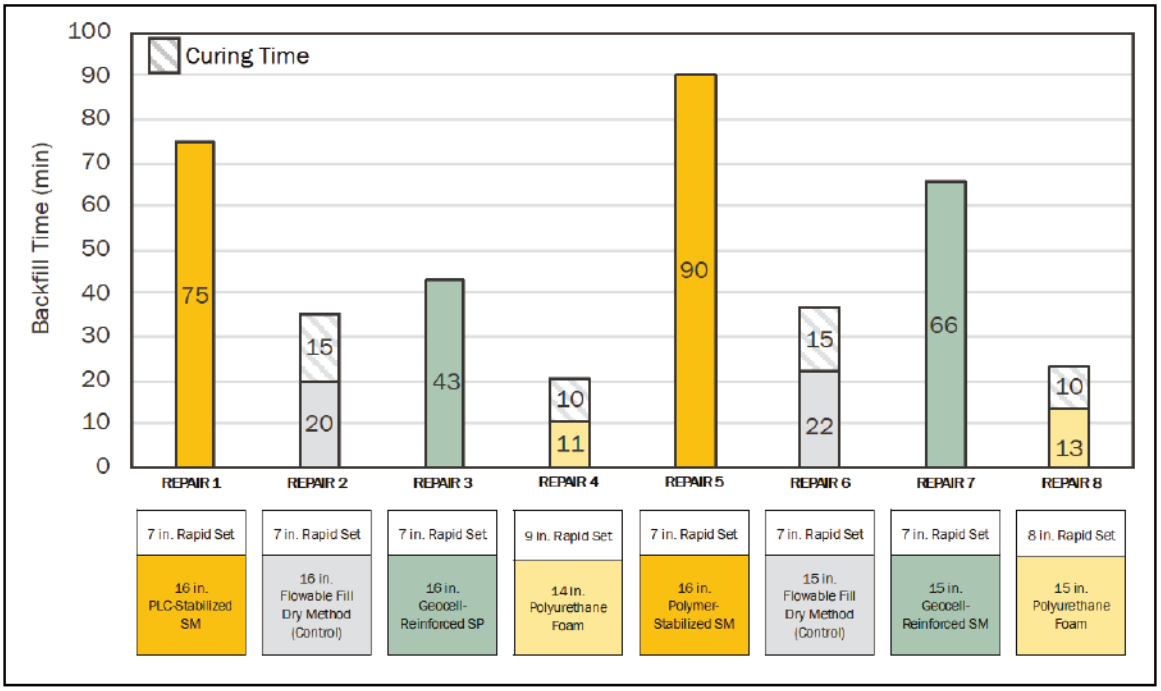

4.3 Post-traffic results

4.3.1 Pavement distress survey

A summary of the condition and distress data collected throughout trafficking is provided in Appendix C. The results of the pavement condition for all repairs are reported in Figure 4.2. The repairs withstood varying levels of traffic prior to failing. The repairs with cement-stabilized SM and rapid-setting flowable fill (Repairs 1, 2, and 6) met the RADR objective pass level for sustainment level repairs. These did not fail, but trafficking was stopped at 3,600 passes. The remaining repairs sustained at least 500 passes, therefore meeting the RADR threshold pass level for expedient repairs. The geocell-reinforced SM and the polymer-stabilized SM were the best performers in this category. Some repairs were trafficked after failure was identified to capture additional data.

Figure 4.2. Traffic data summary.

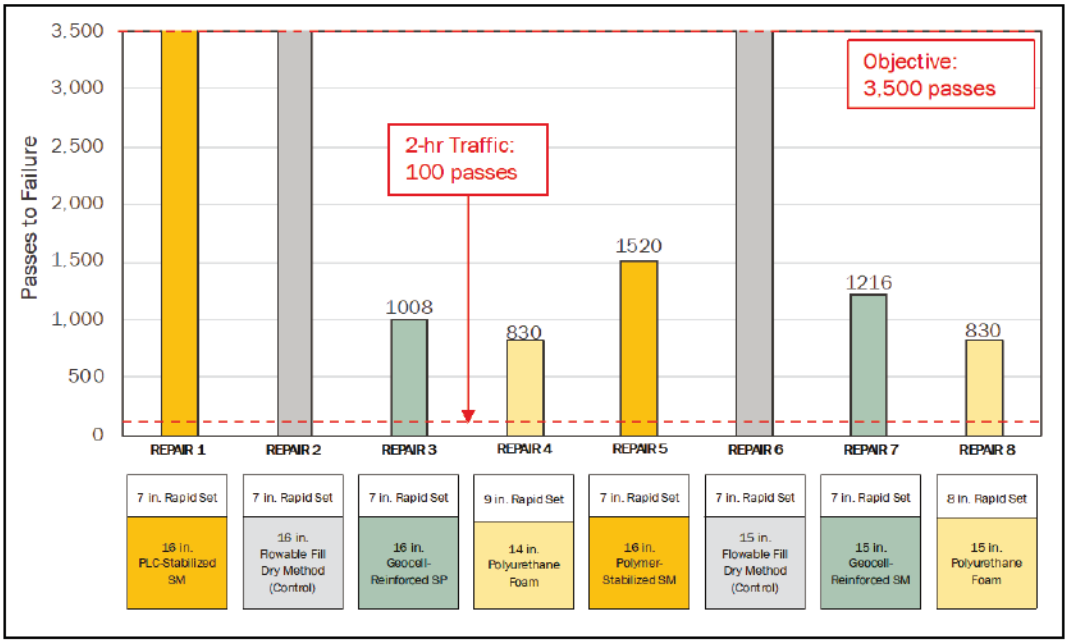

The main mode of failure was high-severity spalling along the transverse joints (perpendicular to the direction of traffic). Minor distresses, such as shrinkage cracking after curing, were noted prior to traffic for many of the repairs but did not appear to contribute to their failures. Figures 4.3 through 4.10 show post-traffic photos for each repair. Figure 4.11 shows shrinkage cracking on Repair 4 prior to trafficking (marked with orange paint stick).

Figure 4.3. Post-traffic photographs of Repair 1 after 3,600 passes.

Figure 4.4. Post-traffic photographs of Repair 2 after 3,600 passes.

Figure 4.5. Post-traffic photographs of Repair 3 after 1,520 passes.

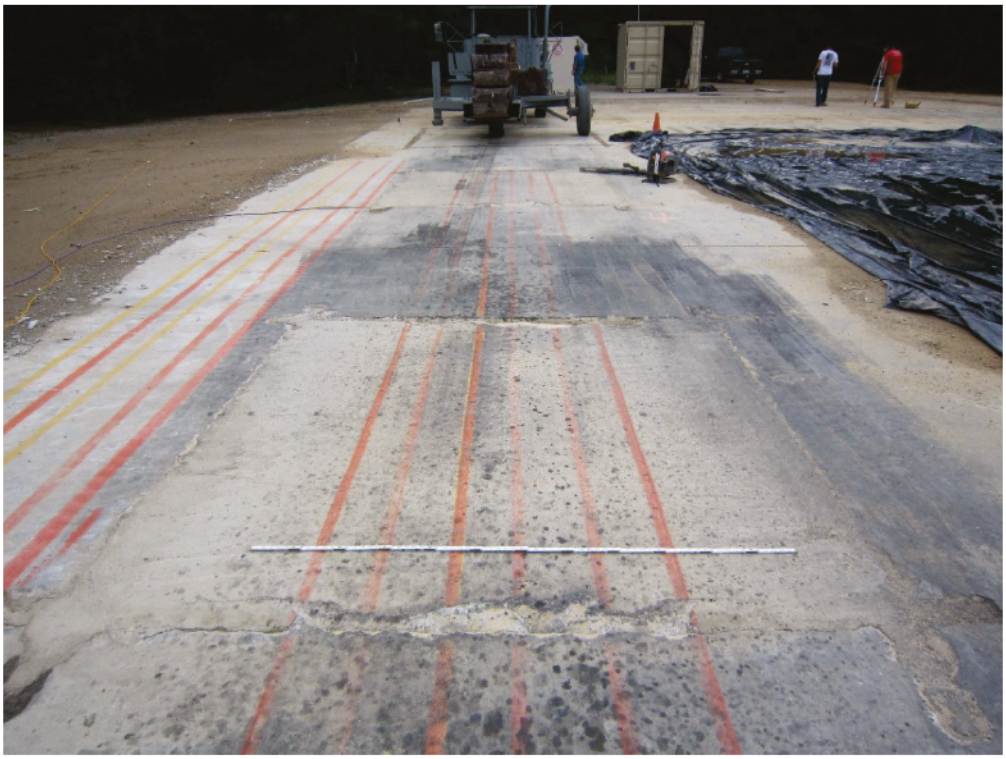

Figure 4.6. Post-traffic photographs of Repair 4 after 830 passes.

Figure 4.7. Post-traffic photographs of Repair 5 after 1,520 passes.

Figure 4.8. Post-traffic photographs of Repair 6 after 3,600 passes.

Figure 4.9. Post-traffic photographs of Repair 7 after 1,792 passes.

Figure 4.10. Post-traffic photographs of Repair 8 after 1,520 passes.

Figure 4.11. Shrinkage cracks on Repair 4.

4.3.2 Elevation changes

Permanent deformation and changes at the joint due to removal of spalled material were monitored using rod and level measurements in the longitudinal and transverse directions. Maximum measured changes in elevations for each repair are reported in Table 4.2. The maximum change in elevation was recorded for all repairs along the edges where spalls were located (either on the West or East edges). Note that the values in Table 4.2 are less than that measured during the inspection process with a ruler, which are reported in Appendix C. This is because of the inability to place the rectangular base of the rod in the deepest portions of the spalled areas.

However, Repairs 4, 5, 7, and 8 have maximum changes in elevation that are greater than 1.25 in., which can result in gear damage for the F-15E aircraft. This generally matches the information in Figure 4.2, where these repairs failed by high-severity spalling before reaching 3,600 passes. Repairs 1, 2, and 6 were the best performers and had the lowest values for maximum change in elevation. The survey data also show that there was no evidence of settlement or faulting within the repairs.

Table 4.2. Maximum changes in elevation.

Repair No.	Backfill Type	Pass No.	Max Change in Elevation (in.)	Location of Max Elevation Change
1	Cement-Stabilized SM	3,600	0.48	West
2	Flow Fill	3,600	0.36	West
3	Geocell-Reinforced SP	1,520	1.08	West
4	Foam	830	1.56	East
5	Polymer-Stabilized SM	3,600*	1.32	West
6	Flowable Fill	3,600	0.48	West and East
7	Geocell-Reinforced SM	1,792*	1.80	West
8	Foam	1,520*	1.92	West

*Survey data was only taken when traffic was discontinued on each repair and not necessarily when the repair was considered failed.

4.3.3 Impact stiffness modulus

Figure 4.12 shows the impact stiffness modulus (ISM) results obtained from the FWD test data. The plot shows that the repairs lost about 50% of the stiffness at around 1,000 passes.

Figure 4.12. FWD results.

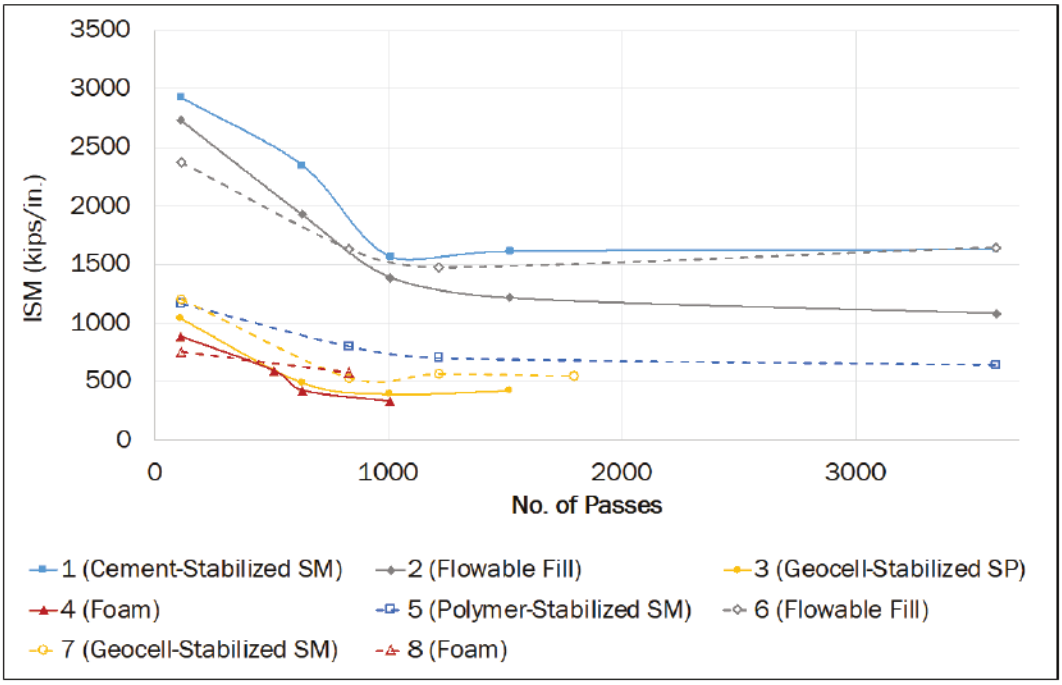

After that point, the ISM values stabilized, and no significant change was observed. Repairs with cement-stabilized soil and flowable fill backfills had similar trends and were the stiffest compared to the rest of the repairs. This was expected, considering the cementitious nature of the flowable fill and cement-stabilized materials. The polymer emulsion-stabilized SM showed a slightly higher stiffness than the geocell-reinforced repairs. However, it showed a much lower stiffness than the PLC-stabilized repair. For the geocell-reinforced repairs, Repair 7, which was backfilled with SM soil, was stiffer than Repair 3, which was backfilled with a uniform SP soil.

4.3.4 Earth pressure cell data

Table 4.3 shows a summary of the average peak pressures measured below the backfill in each repair. Figures 4.13 and 4.14 present the peak pressures measured during each traffic interval applied to the repairs. Each traffic interval represents a different day when traffic was applied with the load cart. Before traffic began each day, the data collection system was turned on and the initial pressure values were recorded. These pressures were then used to baseline the data to account only for the pressure effects on the EPCs caused by the applied traffic and, thus, to neglect the overburden pressures caused by the weight of the backfill and capping layers.

Table 4.3. Average peak pressures measured on each repair.

Repair No.	Backfill Technology	Average Peak Pressure (psi)	Standard Deviation
1	Cement-Stabilized SM	4.9	1.1
2	Flowable Fill	3.1	1.2
3	Geocell with SP	1.3	0.6
4	Foam	2.0	0.9
5	Polymer-Stabilized SM	8.4	1.7
6	Flowable Fill	2.7	1.1
7	Geocell with SM	3.7	1.6
8	Foam	3.0	1.5

Figure 4.13. Peak pressure values for Repairs 1 through 4 during each pass interval applied.

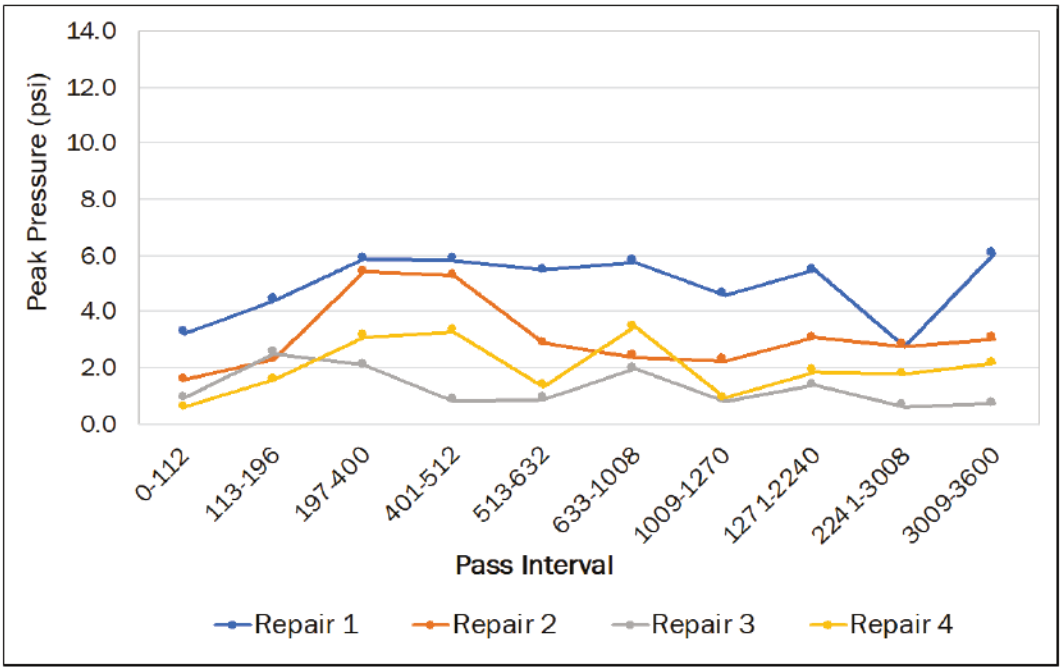

It is important to note that data from Repairs 5 through 8 during passes 0 through 200 are not available due to technical issues with the instrumentation, as shown in Figure 4.14.

In general, the data show significantly low pressures (less than 10 psi) below the backfill layer across all repairs. This indicates that most of the pressure applied by the simulated F-15 traffic was well-dissipated by the

rapid-setting concrete cap and the backfill. The pressures measured were generally consistent during traffic for most of the repairs.

Figure 4.14. Peak pressure values for Repairs 5 through 8 during each pass interval applied.

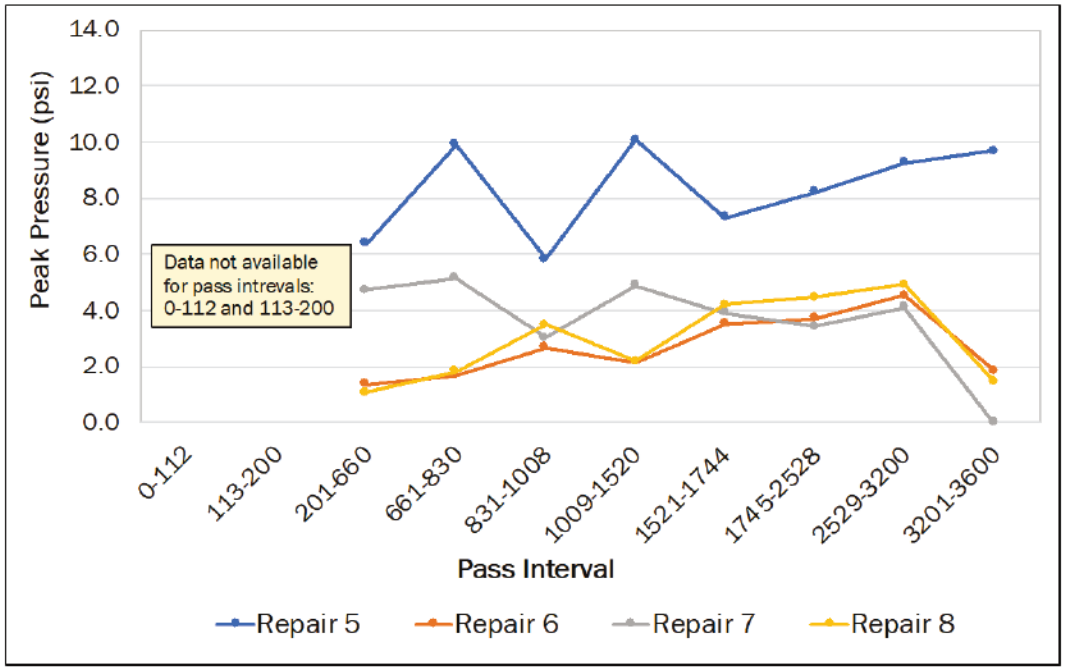

Some of the changes in observed pressure were attributed to instrumentation technical issues rather than to repair failure. Since the traffic was applied in an alternate pattern between the two test sequences, the data collection system was moved back and forward to capture the EPC readings during traffic at each test sequence. This resulted in inconsistent baseline pressure values due to inherent equipment error.

It was observed that Repairs 1 and 5 had the highest overall pressures measured. These were the cement- and polymer-stabilized soils. The high pressure could be attributed to the fact that these stabilization methods required longer curing times.

5 Comparison of Backfill Technologies

The test observations indicated that the rapid-setting flowable fill and cement-stabilized soil backfills met the RADR objective of 3,500 passes under a 7-in.-thick rapid-setting concrete cap. However, for the geocell and foam backfills the 7-in.-thick cap was not adequate, as these repairs did not reach the 3,500-passes RADR objective. It is recommended to use the foam backfill technology with a minimum rapid-setting concrete cap thickness of 10 in. (Johnson et al. 2017; Priddy et al. 2016; Bell et al. 2019; Mejias-Santiago et al. draft*). Further research is required to characterize the geocell-reinforced backfill performance with a 10-in.-thick rapid-setting concrete cap.

In general, the experiment observations and results indicated that the three backfill technologies evaluated have potential for use in RADR. Each technology has trade-offs, and their applicability will depend on the RADR operation scenario. For comparison purposes, a trade-off analysis was conducted to determine the rankings of all backfill technologies evaluated. The criteria used for the analysis included repair logistics (such as equipment, materials, manpower, and repair times, repair performance under simulated aircraft traffic, and material costs). The rapid-setting flowable fill backfill technology was included in this analysis for comparison purposes. Each technology received a ranking value from 1 to 4, where a ranking of 4 means that technology is the best of the four in that specific parameter.

Table 5.1 presents the results of the trade-off analysis. On average, all four technologies share similar rankings. The use of each individual technology depends on the RADR scenario and the availability of backfill materials. For example, the best performing material under simulated aircraft traffic is the rapid-setting flowable fill. If there were access to take the material in to the RADR location, the recommended backfill technology would be rapid-setting flowable fill. This is the current backfill technology used for RADR, but its limitation is the material footprint and weight. A lighter solution in this case would be the foam backfill technology. However, it needs to be understood that this technology requires specialized equipment and training. In the case where there is no access to take in

* Mejias-Santiago, M., J. S. Tingle, J. L. Johnson, L. A. Gurtowski and C. S. Griggs. Draft. *Refinement of foam backfill technology for expedient airfield damage recovery Phase III: Technology demonstration and end user evaluation*. ERDC/GSL TR. Vicksburg, MS: U.S. Army Engineer Research and Development Center.

materials and indigenous materials are to be used, cement-stabilized soil would be the recommended backfill technology. Cement is cheap, and it is generally available in most countries. However, the soil-stabilization process is labor-intensive and time-consuming. A quicker approach for stabilizing indigenous materials would be using geocells for mechanical stabilization. The geocells are lightweight and easy to transport and store. Furthermore, UFC 3-270-07 allows the use of FOD cover in combination with geocells for expedient repairs, requiring a much smaller logistical footprint than rapid-setting concrete. Using a FOD cover requires less material and less specialized equipment than rapid-setting concrete, which utilizes a volumetric mixer for placement.

Table 5.1. Technology trade-off analysis.

Parameter	Requirement	Flowable Fill	Cement-Stabilized Soil	Geocells	Foam
Repair Logistics	Equipment Materials Manpower Repair Time	4 1 3 3	2 3 2 1	3 4 1 2	1 2 4 4
Repair Performance	2-hr Traffic: 100 passes Objective: 3,500 passes	4 4	4 3	4 2	4 1
Material Cost[a]	8.5 ft x 8.5 ft x 16 in. backfill	1	4	3	2
	Average Ranking:	2.9	2.7	2.7	2.6

[a] Material costs for 16 in. of backfill in one small crater (96 ft³):

flowable fill: $3,200

cement: $100

geocells: $600

foam: $3,100

6 Conclusions and Recommendations

This experiment evaluated three different crater backfill technologies during a full-scale field experiment to compare their performances and conduct a technology trade-off analysis. The technologies evaluated included (1) expandable polyurethane foam, (2) mechanical soil reinforcement, and (3) chemical soil stabilization. After the repairs were completed, simulated F-15E aircraft traffic was applied to the repairs to verify their ability to meet the operational RADR mission requirements. Detailed performance data were gathered in terms of timing, manpower requirements, and logistical requirements to support a trade-off analysis of these technologies.

The following conclusions and recommendations were determined from the experiment and trade-off analysis.

6.1 Conclusions

1. All of the backfill tested demonstrated an ability to support aircraft traffic. Each technology has trade-offs, and their applicability will depend on the RADR scenario.
2. The foam backfill technology required the least manpower, time, and logistical footprint of all backfill methods evaluated in this experiment. However, repairs with foam backfill did not meet the 3,500-pass sustainment level requirement for RADR. Foam backfill technology provides a small logistical footprint, but it requires specialized equipment and training.
3. A layer of 16 in. of compacted silty sand stabilized with 5% cement is a backfill material comparable to rapid-setting flowable fill for 3,500 simulated F-15E passes under a 7-in.-thick rapid-setting concrete cap. The cement-stabilized soil and rapid-setting flowable fill backfill were placed on the same day during this testing and were allowed to cure for approximately 4 hr prior to trafficking the initial 112 passes after cap placement. While the time to mix and place the cement-stabilized backfill was longer, the cement-stabilized soil can be used when flowable fill is not available. This method requires less added material but an available source of soil.
4. This experiment provided new information on the performance of geocell-reinforced soil under a rapid-setting concrete cap. The repair with the geocell-reinforced silty-sand backfill performed well under simulated F-15E traffic but did not meet the sustainment-level

performance requirements under 7 in. of rapid-setting concrete cap. Geocells provide a small logistical footprint but require significantly more manpower for installation than other backfill repair methods described in this report.

5. Data indicated that SM soil stabilization using cement produced a better quality backfill than when polymer or geocells were used to stabilize the same SM soil.

6.2 Recommendations

1. Only the rapid-setting flowable fill and cement-stabilized soil backfills are recommended for crater repairs with a 7-in. rapid-setting concrete cap thickness to meet the sustainment-level RADAR performance requirement (3,500 passes). The minimum rapid-setting concrete cap thickness recommended for geocell and foam backfills is 10 in.
2. For cement-stabilized silty sand, the moisture of the soil should be on the wet side with up to 10% moisture content. If not enough moisture is present, water can be added when compacting. The lack of adequate water content causes problems in achieving a good compaction and also may not provide enough moisture for hydration of PLC.

References

Air Force Civil Engineer Center (AFCEC). 2012. *Repair of cement-stabilized soil surfaces*. Engineering Technical Letter, ETL 12-7. Panama City, FL: Tyndall AFB.

Air Force Civil Engineer Center (AFCEC). 2018. *Interim tactics, techniques, and procedures (TTP), interim process for Rapid Airfield Damage Recovery (RADR)*. Revision 11.2. Panama City, FL: Tyndall AFB.

American Society for Testing and Materials International (ASTM). 2018. *Standard test method for use of the dynamic cone penetrometer in shallow pavement applications*. Designation: D6951. West Conshohocken, PA: American Society for Testing and Materials.

ASTM International. 2015a. *Standard test method for measuring deflections with a light weight deflectometer (LWD)*. Designation: E2583-07. West Conshohocken, PA: American Society for Testing and Materials.

ASTM International. 2015b. *Standard test method for measuring deflections using a portable impulse plate load test device*. Designation: E2835-11. West Conshohocken, PA: American Society for Testing and Materials.

_____. 2017a. *Standard practice for classification of soils for engineering purposes (Unified Soil Classification System)*. Designation: D2487. West Conshohocken, PA: American Society for Testing and Materials.

_____. 2017b. *Standard test methods for in-place density and water content of soil and soil-aggregate by nuclear methods (shallow depth)*. Designation: D6938. West Conshohocken, PA: American Society for Testing and Materials.

_____. 2019. *Standard specification for blended hydraulic cements*. Designation: C595. West Conshohocken, PA: American Society for Testing and Materials.

Bell, H. P., L. Edwards, W. D. Carruth, J. S. Tingle, and J. R. Griffin. 2013. *Wet weather crater repair testing at Silver Flag exercise site, Tyndall Air Force Base, Florida*. ERDC/GSL TR-13-42. Vicksburg, MS: U.S. Army Engineer Research and Development Center.

Bell, H. P., B. C. Cox, L. Edwards, L. I. Garcia, N. R. Hoffman, M. Mejias-Santiago, and J. L. Johnson. 2019. *Rapid airfield damage recovery technology integration experiment*. ERDC/GSL TR-19-8. Vicksburg, MS: U.S. Army Engineer Research and Development Center.

Carruth, W. D., L. Edwards, H. P. Bell, J. S. Tingle, J. R. Griffin, and C. A. Rutland. 2015. *Large crater repair at Silver Flag exercise site, Tyndall Air Force Base, Florida*. ERDC/GSL TR-15-27. Vicksburg, MS: U.S. Army Engineer Research and Development Center.

Concrete Construction. 2014. The advantages of Portland-limestone cement. http://www.theconcreteproducer.com/how-to/concrete-production.

Department of the Army, the Navy, and the Air Force. 2003. *Airfield damage repair*. Unified Facilities Criteria UFC 3-270-07. Washington, DC: Department of the Army, Navy, and Air Force.

_____. 2004. *Soil stabilization for pavements*. Unified Facilities Criteria UFC 3-250-11. Washington, DC: Department of the Army, Navy, and Air Force.

Edwards, L., H. P. Bell, W. D. Carruth, J. R. Griffin, and J. S. Tingle. 2013. *Cold weather crater repair testing at Malmstrom Air Force Base, Montana*. ERDC/GSL TR-13-32. Vicksburg, MS: U.S. Army Engineer Research and Development Center.

Gurtowski. L., M. Mejias-Santiago, C. Griggs, J. Johnson, B. Ruiz, and D. Felt. 2016. *Refinement of foam backfill technology for expedient airfield damage recovery Phase I: Laboratory evaluation of foam materials*. ERDC/GSL TR-16-16. Vicksburg, MS: U.S. Army Engineer Research and Development Center.

Johnson, J. L., M. Mejias-Santiago, L. A. Gurtowski, C. Griggs, and C. A. Rutland. 2017. *Refinement of foam backfill technology for expedient airfield damage recovery Phase II: Development of prototype foam dispensing equipment and improved tactics, techniques and procedures*. ERDC/GSL TR-17-14. Vicksburg, MS: U.S. Army Engineer Research and Development Center.

Johnson, J. L., C. A. Weiss, L. Edwards, J. S. Tingle, W. S. Hammond, and T. J. Talbot. 2018. *Laboratory evaluation of next-generation backfill materials and methods for airfield damage repair*. ERDC/GSL TR-18-33. Vicksburg, MS: U.S. Army Engineer Research and Development Center.

Priddy, L. P., H. P. Bell, L. Edwards, W. D. Carruth, and J. F. Rowland. 2016. *Evaluation of the structural performance of CTS Rapid Set Concrete Mix®*. ERDC/GSL TR-16-20. Vicksburg, MS: U.S. Army Engineer Research and Development Center.

Priddy, L. P., J. S. Tingle, M. C. Edwards, J. R. Griffin, and T. J. McCaffrey. 2013. *CRATR technology demonstration: Limited operational utility assessment 2, Tyndall Air Force Base, Florida*. ERDC/GSL TR-13-39. Vicksburg, MS: U.S. Army Engineer Research and Development Center.

Read, D. L., and P. E. Dukes. 1988. *Sand grid base course Phase I, for fiberglass mat crater repair*. Report RRR-TR-88-01. Tyndall Air Force Base, FL: The Air Force Engineering and Services Center.

Stamp, D., and M. Mooney. 2013. Influence of lightweight deflectometer characteristics on deflection measurement. *Geotechnical Testing Journal* 36(2).

Tingle, J. S., L. P. Priddy, M. C. Edwards, C. A. Gartrell, and T. J. McCaffrey. 2009. *Critical runway assessment and repair (CRATR) technology demonstration: Limited operational utility assessment 1 (LOUA1), Tyndall Air Force Base, Florida*. ERDC/GSL TR-09-12. Vicksburg, MS: U.S. Army Engineer Research and Development Center.

United States Air Force (USAF). 1992. *Crushed-stone cater repair and line-of-sight profile measurement for rapid runway repair*. TO 35E2-5-1. Washington, DC: USAF.

Webster, S. L. 1986. *Sand-grid demonstration roads constructed for JLOTS II tests at Fort Story, Virginia*. Technical Report GL-86-19. Vicksburg, MS: U.S. Army Engineer Waterways Experiment Station.

Appendix A: Constructed Subgrade Soil Classification Data

Silty Clay (CL-ML)

LIQUID LIMIT, PLASTIC LIMIT, AND PLASTICITY INDEX OF SOILS

ASTM D 4318

WORK ORDER NO. EP1728 DATE 7/13/2017

PROJECT Next Generation Backfill

BORING NO. ERDC Stockpile SAMPLE NO. Silt 1

LIQUID LIMIT

Run No.	1	2	3	4	5	6	7
Tare No.	15J	52	40	92			
Tare Plus Wet Soil, g	32.03	33.36	35.47	28.63			
Tare Plus Dry Soil, g	28.15	29.17	30.77	25.46			
Water, g	3.88	4.19	4.70	3.17			
Tare, g	15.24	15.35	15.51	15.29			
Dry Soil, g	12.91	13.82	15.26	10.17			
Water content, %	30.1	30.3	30.8	31.2			
Number of Blows	34	28	21	16			

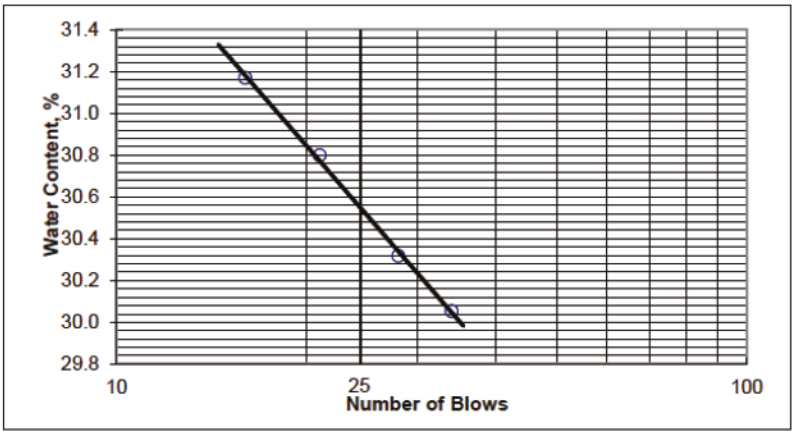

LL 31
PL 25
PI 6

Symbol from plasticity chart: CL-ML

Plastic LIMIT

Run No.	1	2	3	4	5	6	7
Tare No.	112	135C					
Tare Plus Wet Soil, g	32.64	56.00					
Tare Plus Dry Soil, g	29.26	52.02					
Water, g	3.38	3.98					
Tare, g	15.52	35.91					
Dry Soil, g	13.74	16.11					
Water content, %	24.6	24.7					
Plastic Limit	24.7						

Remarks Silty Clay (CL-ML), Brown

Technician AT Computed By AT Checked By TRJ

Revised 5/21/09

LIQUID LIMIT, PLASTIC LIMIT, AND PLASTICITY INDEX OF SOILS

ASTM D 4318

WORK ORDER NO. EP1728 DATE 7/13/2017

PROJECT Next Generation Backfill

BORING NO. ERDC Stockpile SAMPLE NO. Silt 2

LIQUID LIMIT

Run No.	1	2	3	4	5	6	7
Tare No.	373	396	402	478			
Tare Plus Wet Soil, g	34.15	34.35	33.01	32.63			
Tare Plus Dry Soil, g	29.76	29.88	29.05	28.64			
Water, g	4.39	4.47	3.96	3.99			
Tare, g	14.96	15.11	16.11	15.76			
Dry Soil, g	14.80	14.77	12.94	12.88			
Water content, %	29.7	30.3	30.6	31.0			
Number of Blows	34	28	23	18			

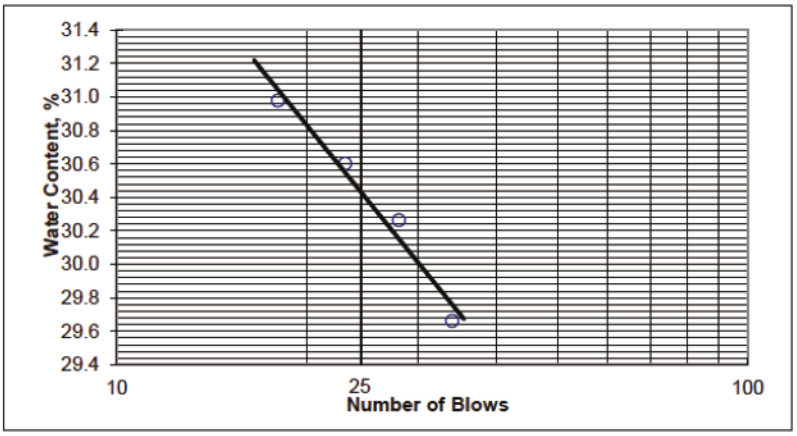

LL 30
PL 23
PI 7

Symbol from plasticity chart: CL- ML

Plastic LIMIT

Run No.	1	2	3	4	5	6	7
Tare No.	494	516					
Tare Plus Wet Soil, g	36.85	35.62					
Tare Plus Dry Soil, g	32.82	31.78					
Water, g	4.03	3.84					
Tare, g	15.57	15.40					
Dry Soil, g	17.25	16.38					
Water content, %	23.4	23.4					
Plastic Limit	23.4						

Remarks Silty Clay (CL-ML), Brown

Technician AT Computed By AT Checked By TRJ

Revised 5/21/09

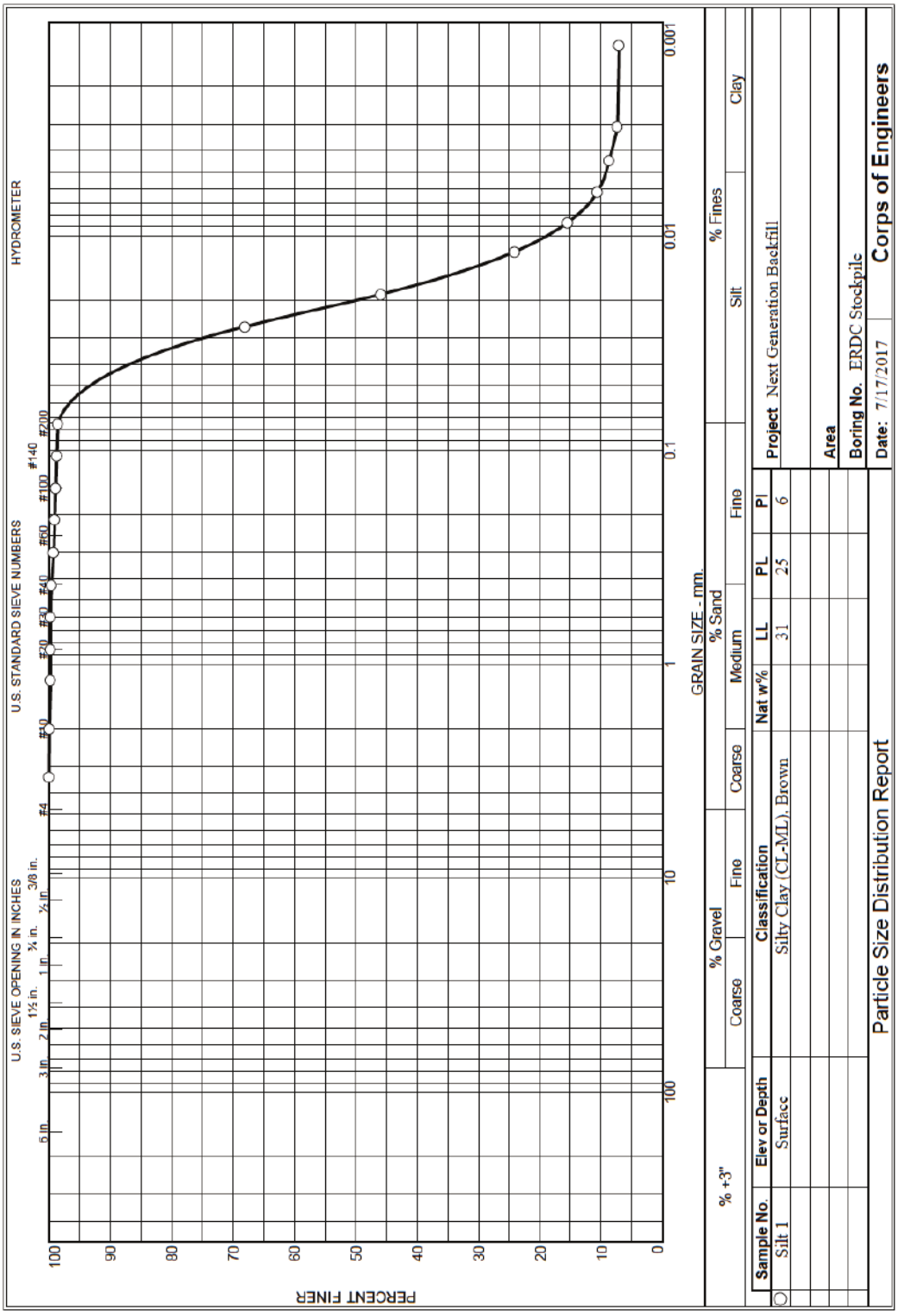
U.S. SIEVE OPENING IN INCHES
U.S. STANDARD SIEVE NUMBERS
HYDROMETER
PERCENT FINER
GRAIN SIZE - mm.
% +3"
% Gravel
% Sand
% Fines
Coarse
Fine
Coarse
Medium
Fine
Silt
Clay
Sample No. Elev or Depth Classification Nat w% LL PL PI
Silt 1 Surface Silty Clay (CL-ML), Brown 31 25 6
Project Next Generation Backfill
Area
Boring No. ERDC Stockpile
Date: 7/17/2017
Particle Size Distribution Report
Corps of Engineers
ENG FORM 1 MAY 63 2087

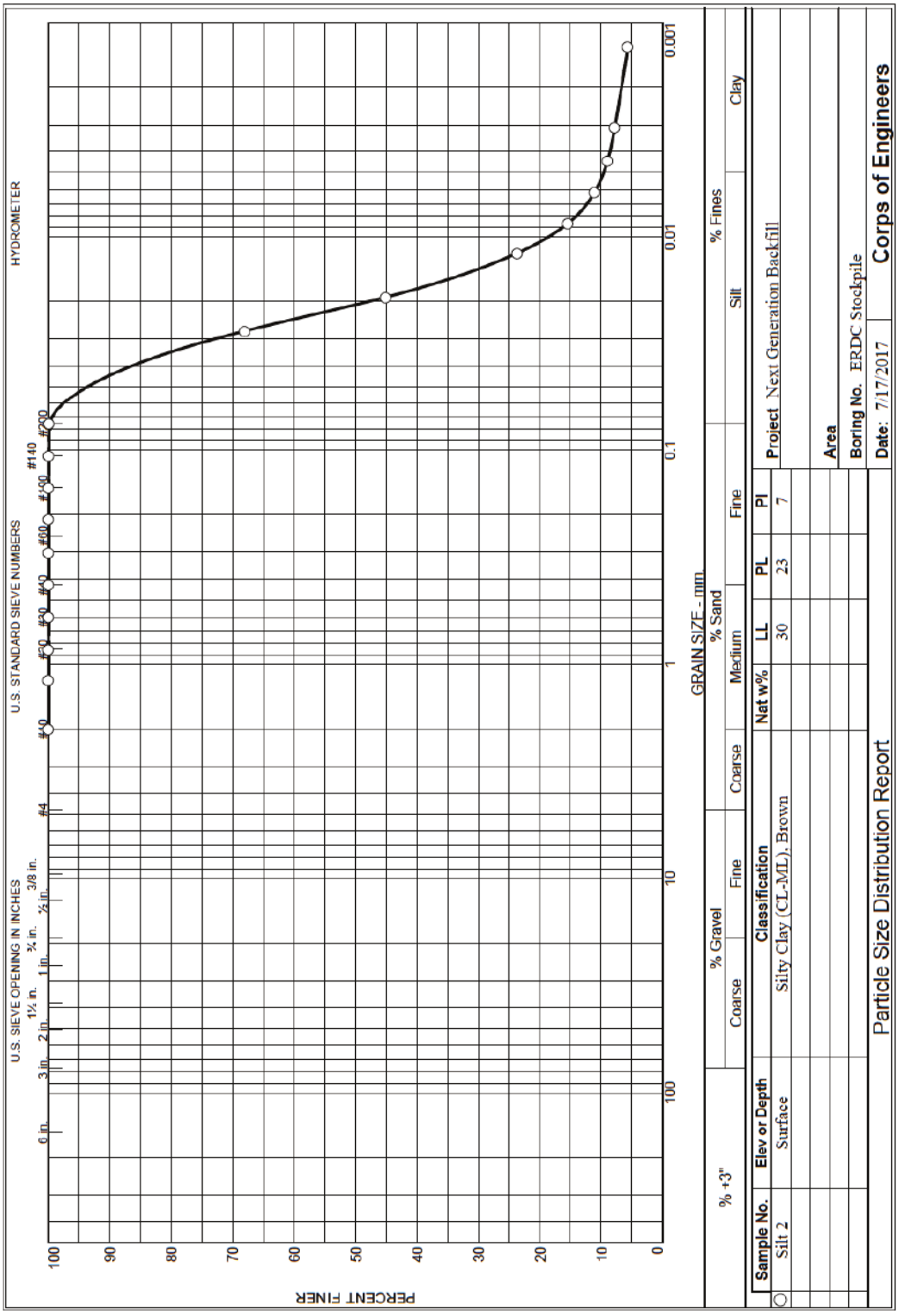

ENG FORM 1 MAY 63 2087

SPECIFIC GRAVITY OF SOILS
ASTM D 854
FLASK SET # 1

WORK ORDER NO. EO1728 Date: 7/10/17
Project: Next Generation Backfill

Method A: _____ Method B: X

Boring:	ERDC Stockpile		ERDC Stockpile	
Location:				
Sample No.:	Silt 1		Silt 2	
Flask No.:	12	16	28	32
Weight dry soil after test, g, (M_s) :	66.33	65.15	70.35	66.89
Test temp., °C:	25.6	25.4	26.2	26.3
Average calibrated weight of flask, g, (M_p):	167.30	173.12	169.33	169.90
Average calibrated volume of flask, ml, (Vp):	499.41	499.32	499.39	499.42
Weight of flask, water, & soil @ test temp., g, ($M_{pws,t}$):	707.52	712.54	712.00	710.62
Density of water @ test temp., g/ml, (Table 1, ($P_{w,t}$)):	0.99690	0.99695	0.99674	0.99671
Temp. coefficient, (Table 1 (K)) :	0.99869	0.99874	0.99853	0.99850
$M_{pw,t}$ =	665.16	670.92	667.09	667.68
G_t =	2.77	2.77	2.77	2.79
$G_{20°C}$ =	**2.76**	**2.77**	**2.76**	**2.79**
Average $G_{20°C}$ =	**2.76**		**2.78**	

Formulas: Weight of flask & water @ test temp., g = $M_{pw,t} = M_p + (V_p \times P_{w,t})$
Specific gravity of soil @ test temp. = $Gt = M_s/(M_{pw,t} - (M_{pws,t} - M_s))$
Specific gravity of soil @ 20°C = $K \times G_t$

Visual Classification:	Silty Clay (CL-ML), Brown	Silty Clay (CL-ML), Brown
% passing No. 4 sieve Spl No.:	100	100
Was soil or material excluded?	Yes _____ No	Yes _____ No X
Description material excluded Spl No.:		

Remarks:

Technician: FAN Computed by: FAN Checked by: TRJ

Revised 2/27/17

Appendix B: Backfill Soils' Classification Data

Silty Sand (SM)

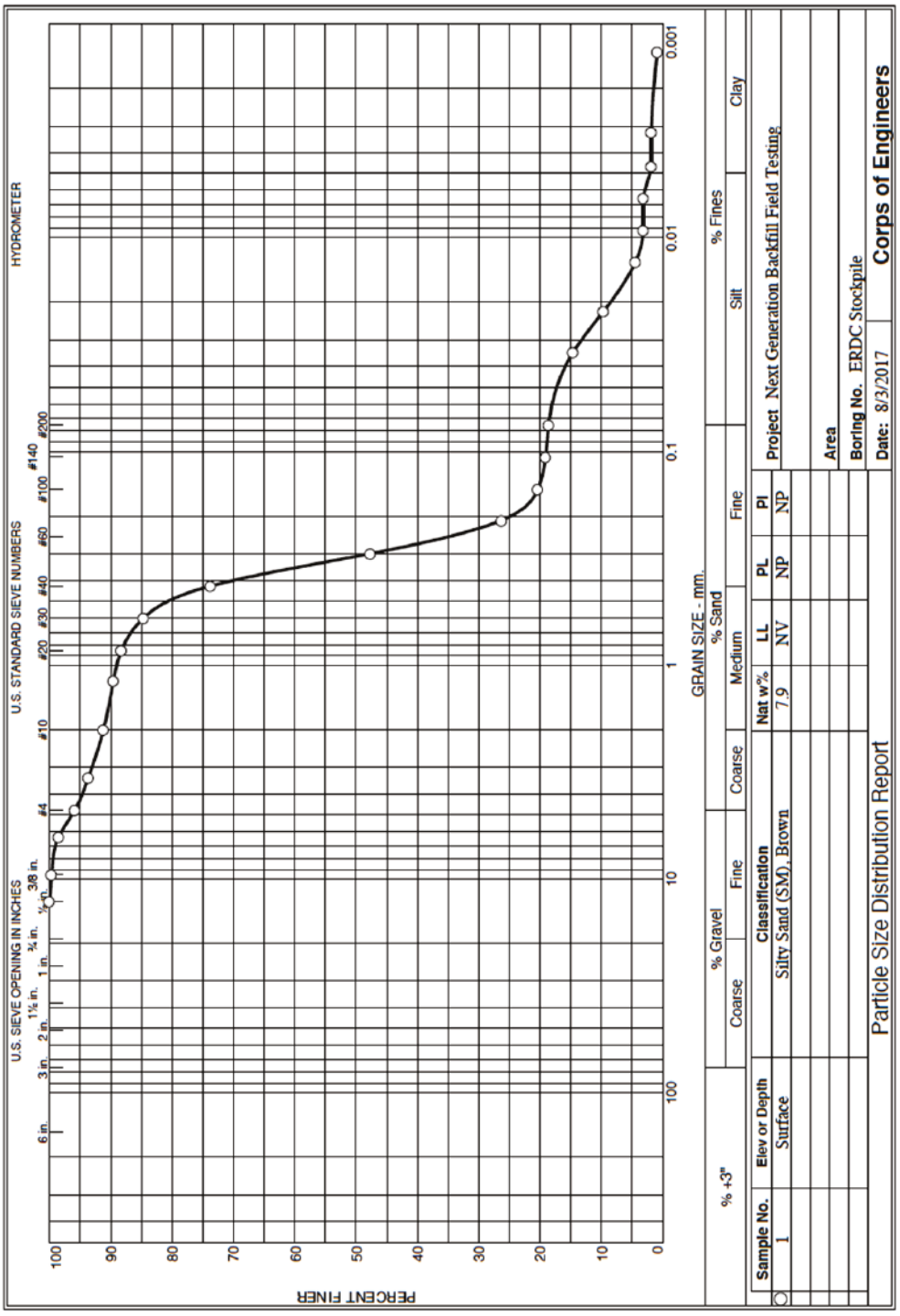

SPECIFIC GRAVITY OF SOILS
ASTM D 854
FLASK SET # 1

WORK ORDER NO. EP1729 Date: 7/21/17

Project: Next Generation Backfill Field Testing

Method A: _____ Method B: X

Boring:	ERDC Stockpile		ERDC Stockpile 2	
Location:				
Sample No.:	Silty Sand 1		Silyt Sand 1	
Flask No.:	12	16	28	32
Weight dry soil after test, g, (M_s) :	103.68	102.62	103.28	99.61
Test temp., °C:	25.3	25.2	25.2	25.1
Average calibrated weight of flask, g, (M_p):	167.30	173.12	169.33	169.90
Average calibrated volume of flask, ml, (Vp):	499.41	499.32	499.39	499.42
Weight of flask, water, & soil @ test temp., g, ($M_{pws,t}$):	730.29	735.31	732.12	730.43
Density of water @ test temp., g/ml, (Table 1, ($P_{w,t}$)):	0.99698	0.99700	0.99700	0.99703
Temp. coefficient, (Table 1 (K)) :	0.99877	0.99879	0.99879	0.99882
$M_{pw,t}$ =	665.20	670.94	667.22	667.84
G_t =	2.69	2.68	2.69	2.69
$G_{20°C}$ =	2.68	2.68	2.69	2.69
Average $G_{20°C}$ =	2.68		2.69	

Formulas: Weight of flask & water @ test temp., g = $M_{pw,t} = M_p + (V_p \times P_{w,t})$

Specific gravity of soil @ test temp. = $Gt = M_s/(M_{pw,t} - (M_{pws,t} - M_s))$

Specific gravity of soil @ 20°C = $K \times G_t$

Visual Classification:	Silty Sand (SM), Brown	Silty Sand (SM), Brown
% passing No. 4 sieve Spl No.:		
Was soil or material excluded?	Yes _____ No X	Yes _____ No X
Description material excluded Spl No.:		

Remarks: _____

Technician: FAN Computed by: FAN Checked by: TRJ

Revised 2/27/17

COMPACTION TEST REPORT

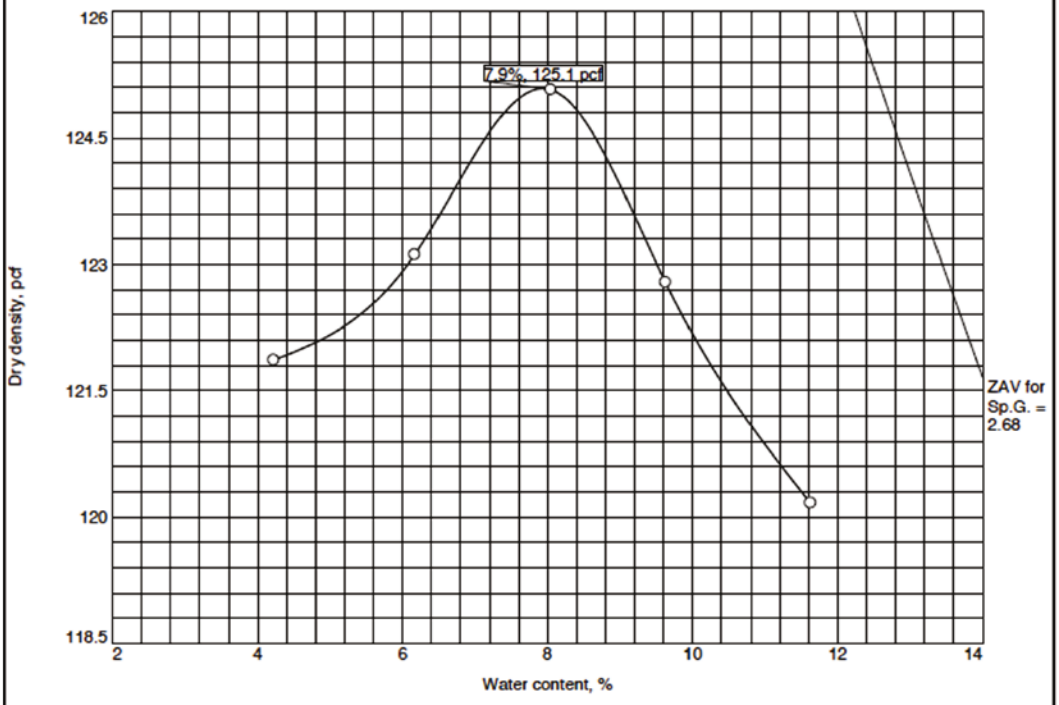

ASTM D 1557-12 Method B Modified

25 blows per each of 5 layers, with 10 lb. rammer and 18 in. drop. 0.03333 cu. ft. mold.

Elev/ Depth	Classification		Nat. Moist.	Est. Sp.G.	LL	PL	% > 3/8 in.	% < No.200
	USCS	AASHTO						
Surface	Silty Sand (SM)		7.9	2.68	NV	NP	0.4	18.6

TEST RESULTS	MATERIAL DESCRIPTION
Optimum moisture = 7.9 % Maximum dry density = 125.1 pcf	ERDC Stockpile Silty Sand 1

Project: Next Generation Backfill Field Testing **Boring No:** **Location:** **Depth or Elevation:** Surface **Date:** 07/27/2017	**Remarks:**
Corps of Engineers **Engineer Research Development Center**	**Figure**

Poorly graded sand (SP)

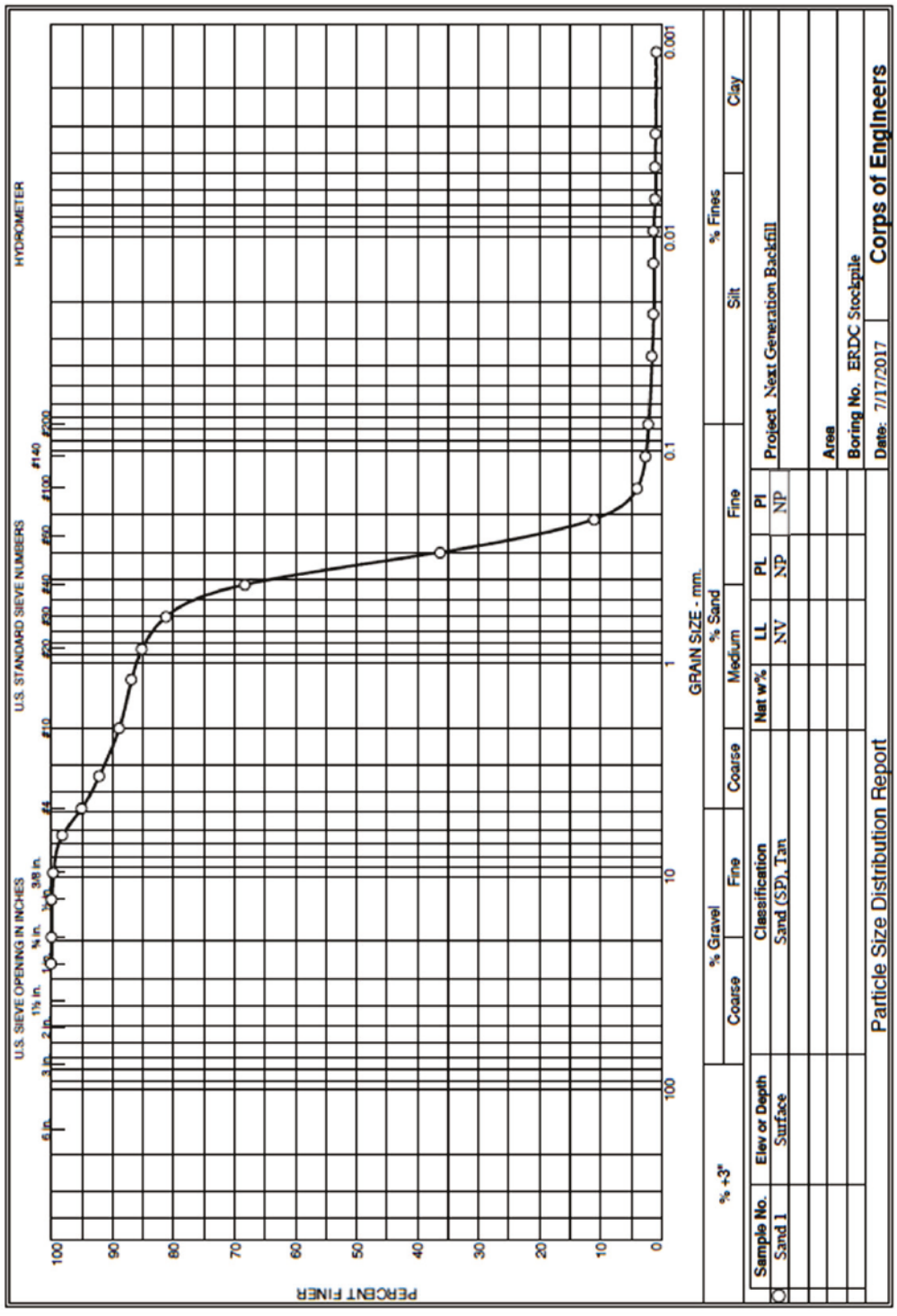

SPECIFIC GRAVITY OF SOILS
ASTM D 854
FLASK SET # 1

WORK ORDER NO. EO1728 Date: 7/12/17

Project: Next Generation Backfill

Method A: Method B: X

Boring:	ERDC Stockpile		ERDC Stockpile	
Location:				
Sample No.:	Sand 1		Sand 2	
Flask No.:	37	40	44	48
Weight dry soil after test, g, (M_s) :	91.24	87.58	111.65	116.69
Test temp., °C:	26.1	26.6	26.4	26.3
Average calibrated weight of flask, g, (M_p):	177.20	174.27	168.88	174.58
Average calibrated volume of flask, ml, (Vp):	499.34	499.44	499.34	499.33
Weight of flask, water, & soil @ test temp., g, ($M_{pws,t}$):	731.98	726.81	736.27	745.13
Density of water @ test temp., g/ml, (Table 1, ($P_{w,t}$)):	0.99677	0.99663	0.99669	0.99671
Temp. coefficient, (Table 1 (K)) :	0.99856	0.99842	0.99848	0.99850
$M_{pw,t}$ =	674.92	672.03	666.56	672.27
G_t =	2.67	2.67	2.66	2.66
$G_{20°C}$ =	**2.67**	**2.67**	**2.66**	**2.66**
Average $G_{20°C}$ =	**2.67**		**2.66**	

Formulas: Weight of flask & water @ test temp., g = $M_{pw,t} = M_p + (V_p \times P_{w,t})$

Specific gravity of soil @ test temp. = $Gt = M_s/(M_{pw,t} - (M_{pws,t} - M_s))$

Specific gravity of soil @ 20°C = $K \times G_t$

Visual Classification:	Sand (SP), Tan		Sand (SP), Tan	
% passing No. 4 sieve Spl No.:	95		95.5	
Was soil or material excluded?	Yes		Yes	
	No	X	No	X
Description material excluded Spl No.:				

Remarks:

Technician: FAN Computed by: FAN Checked by: TRJ

Revised 2/27/17

Appendix C: Pavement Distress Data

Repair 1: Cement-stabilized SM

Date	Pass No.	FOD (in.)		Spall - West Edge			Spall - East Edge		
		West Edge	East Edge	Length (in.)	Width (in.)	Depth (in.)	Length (in.)	Width (in.)	Depth (in.)
26-Jul	0	–	–	–	–	–	–	–	–
26-Jul	112	–	–	–	–	–	–	–	–
1-Aug	196	–	–	–	–	–	–	–	–
2-Aug	400	–	–	–	–	–	–	–	–
2-Aug	512	–	–	–	–	–	–	–	–
4-Aug	632	–	–	–	–	–	–	–	–
9-Aug	830	–	–	16	0.75	0.63	–	–	–
9-Aug	1,008	1	–	16.5	1	0.75	–	–	–
11-Aug	1,270	0.375	0.5	22	1.25	1	18	1	1.063
14-Aug	1,520	0.5	0.5	30	1.75	1	50	1.5	1.25
14-Aug	2,240	0.375	0.5	30	1.75	1	52	1.5	1.25
15-Aug	2,528	0.375	0.375	31	1.75	1.125	53	1.50	1.25
15-Aug	3,008	0.375	0.25	31	1.75	1.25	56	1.75	1.25
16-Aug	3,600	0.75	0.5	46.5	6.25	1.5	70	2.25	1.38

Repair 2: Flowable Fill

Date	Pass No.	FOD (in.)		Spall - West Edge			Spall - East Edge		
		West Edge	East Edge	Length (in.)	Width (in.)	Depth (in.)	Length (in.)	Width (in.)	Depth (in.)
26-Jul	0	–	–	–	–	–	–	–	–
26-Jul	112	–	–	–	–	–	–	–	–
1-Aug	196	–	–	–	–	–	–	–	–
2-Aug	400	0.25	–	30	1	0.25			
2-Aug	512	1	0.5	9	2	0.75	4	1	0.25
4-Aug	632	0.50	0.5	10	2.50	1	10	1.5	0.625
9-Aug	830	1	–	14	3.25	1.125	12	0.75	1.25
9-Aug	1,008	1	1.25	15	3.25	1.25	20	1.25	1.25
11-Aug	1,270	0.375	0.125	57	3.25	1.625	34	2	1.25
14-Aug	1,520	0.5	–	57	3.5	1.625	44	1.75	1.375
14-Aug	2,240	0.375	0.375	69	3.5	1.625	53	1.75	1.375
15-Aug	2,528	0.375	0.375	69	3.5	1.625	56	1.75	1.375
15-Aug	3,008	0.375	0.375	69.5	3.5	1.625	56	1.75	1.375
16-Aug	3,600	1	0.75	75	4.38	1.625	59.50	2.5	1.375

Repair 3: Geocell-reinforced SP

Date	Pass No.	FOD (in.)		Spall - West Edge			Spall - East Edge		
		West Edge	East Edge	Length (in.)	Width (in.)	Depth (in.)	Length (in.)	Width (in.)	Depth (in.)
26-Jul	0	–	–	–	–	–	–	–	–
26-Jul	112	–	–	–	–	–	–	–	–
1-Aug	196	–	–	22	0.50	0.13	11	0.25	–
2-Aug	400	1	1.25	47	3	1.25	68	0.25	–
2-Aug	512	1.25	1	40	4	1	43	4	1.50
4-Aug	632	1	1.25	39.50	4	1.25	46	3	1.50
9-Aug	830	0.75	2	44	4.25	1.375	46	3	2.00
9-Aug	1,008	1	1	56	4.25	1.375	40	6.25	2.125
11-Aug	1,270	1.125	1.375	64	5.875	2	65.50	7	2.50
14-Aug	1,520	1	1	66	5.875	2.63	76	7.50	2.50

Repair 4: Foam

Date	Pass No.	FOD (in.)		Spall - West Edge			Spall - East Edge		
		West Edge	East Edge	Length (in.)	Width (in.)	Depth (in.)	Length (in.)	Width (in.)	Depth (in.)
26-Jul	0	–	–	–	–	–	–	–	–
26-Jul	112	–	–	–	–	–	–	–	–
1-Aug	196	–	0.25	15.00	1.50	0.13	52	1	0.13
2-Aug	400	1.50	1.50	16.00	4.00	0.75	42	3.50	1.50
2-Aug	512	1.00	1.00	16.00	4.00	1.00	42	3.50	1.50
4-Aug	632	2.25	2.00	49.50	10.00	1.50	52	3.50	2
9-Aug	830	–	–	65	9.38	2.75	62	2.50	2.75

Repair 5: Polymer-stabilized SM

Date	Pass No.	FOD (in.)		Spall - West Edge			Spall - East Edge		
		West Edge	East Edge	Length (in.)	Width (in.)	Depth (in.)	Length (in.)	Width (in.)	Depth (in.)
28-Jul	0	–	–	–	–	–	–	–	–
28-Jul	112	–	–	–	–	–	–	–	–
2-Aug	200	1.50	1.00	7.00	1.50	0.50	47.00	1.00	0.63
3-Aug	512	0.75	1.50	9.00	3.00	0.75	34.00	4.00	1.25
3-Aug	634	1.00	1.00	32.00	3.50	1.25	36.50	2.00	1.56
3-Aug	660	3.00	–	51.00	3.75	1.50	50.00	5.00	1.50
4-Aug	750	0.75	–	53.00	4.50	1.50	50.00	5.50	1.875
4-Aug	830	0.25	0.25	54.00	4.50	1.50	50.00	5.00	1.875
16-Aug	1,008	0.50	0.25	66.00	55.00	1.25	60.00	6.50	1.875
17-Aug	1,216	0.50	0.50	70.00	5.00	2.00	65.00	6.50	1.88
17-Aug	1,520	0.50	0.50	70.00	7.00	2.00	69.00	7.00	2.63
22-Aug	1,744	0.38	0.38	78.00	7.25	2.38	71.00	7.00	2.75
23-Aug	2,000	0.38	0.38	78.00	7.25	2.38	71.00	7.00	2.75
23-Aug	2,528	0.38	0.38	80.00	8.50	2.38	75.00	7.00	2.75
24-Aug	3,008	0.38	0.38	82.00	9.00	2.38	75.00	7.00	2.75
24-Aug	3,200	0.50	0.38	85.00	9.25	3.00	82.00	7.00	2.75
25-Aug	3,600	0.38	0.38	85.00	9.25	3.00	83.00	7.00	2.75

Repair 6: Flowable fill

Date	Pass No.	FOD (in.)		Spall - West Edge			Spall - East Edge		
		West Edge	East Edge	Length (in.)	Width (in.)	Depth (in.)	Length (in.)	Width (in.)	Depth (in.)
28-Jul	0	–	–	–	–	–	–	–	–
28-Jul	112	–	–	–	–	–	–	–	–
2-Aug	200	0.25	0.50	–	–	–	9	2	0.50
3-Aug	512	–	0.25	–	–	–	9	2	0.75
3-Aug	634	–	0.25	–	–	–	9	2	0.75
3-Aug	660	–	0.25	–	–	–	9	2	0.75
4-Aug	750	1	1	9	1.25	1	30	1	1.375
4-Aug	830	0.25	1	9	1.25	1.125	44	1.13	1.25
16-Aug	1,008	0.50	1	20	4	1.125	45	2	1.25
17-Aug	1,216	0.375	0.375	21	1.25	1	47	1.75	1.25
17-Aug	1,520	0.375	0.375	26	2	1.375	59	3.25	1.50
22-Aug	1,744	0.375	0.375	34	2	1.375	62	3.25	1.625
23-Aug	2,000	0.50	0.50	48	2.125	1.625	64	3.25	1.625
23-Aug	2,528	0.375	0.50	50	2.125	1.625	64	3.25	1.625
24-Aug	3,008	0.50	0.50	68	2.125	1.625	77	3.25	1.625
24-Aug	3,200	0.375	0.375	70	2.125	1.625	77	3.25	1.625
25-Aug	3,600	0.375	0.375	72	2.125	1.625	77	3.25	1.625

Repair 7: Geocell-Reinforced SM

Date	Pass No.	FOD (in.)		Spall - West Edge			Spall - East Edge		
		West Edge	East Edge	Length (in.)	Width (in.)	Depth (in.)	Length (in.)	Width (in.)	Depth (in.)
28-Jul	0	–	–	–	–	–	–	–	–
28-Jul	112	–	–	–	–	–	–	–	–
2-Aug	200		1	17	1	0.25	18	3	0.75
3-Aug	512	1.5	2	29	3	1.5	23	3	1
3-Aug	634	0.5	2	29	3	1.5	40	3	1
3-Aug	660	1	–	32.5	3.25	1.5	42.5	3	1.25
4-Aug	750	1	1	48	4	1.5	72	3.5	1.5
4-Aug	830	1.5	0.5	48	4.25	1.625	73	3.5	1.5
16-Aug	1,008	0.75	0.25	52	4	1.875	73	6	1.5
17-Aug	1,216	0.5	0.5	57	6.5	2.125	78	6.5	1.5
17-Aug	1,520	0.5	0.5	59	7	2.25	78	9	2.625
22-Aug	1,744	0.5	0.5	61	7	2.625	78	12	2.625
23-Aug	1,792	0.5	0.5	64	7.125	2.625	79	12	2.625

Repair 8: Foam

Date	Pass No.	FOD (in.)		Spall - West Edge			Spall - East Edge		
		West Edge	East Edge	Length (in.)	Width (in.)	Depth (in.)	Length (in.)	Width (in.)	Depth (in.)
28-Jul	0	–	–	–	–	–	–	–	–
28-Jul	112	–	–	–	–	–	–	–	–
2-Aug	200	0.25	0.5	9.5	1.5	0.25	24	2.5	0.75
3-Aug	512	1	1	14	2	1	48	3	1
3-Aug	634	1	0.75	31	5.5	1.125	48	3	1.375
3-Aug	660	1		32.5	5.75	1.25	68.5	3	1.375
4-Aug	750	2	0.5	34.5	5.75	1.875	68.5	3	1.5
4-Aug	830	3	1	39.5	10	2.125	52	3	1.5
17-Aug	1,520	0.5	0.5	69	11	2.625	66	6.5	1.875

Acronyms

RADR	Rapid Airfield Damage Recovery
AFCEC	U.S. Air Force Civil Engineer Center
APB	Airfields and Pavements Branch
ERDC	U.S. Army Engineer Research and Development Center
ESMD	Engineering Systems and Materials Division
FOD	foreign object debris
GSL	Geotechnical and Structural Laboratory
hr	Hour
min	Minute
pcf	pounds per cubic foot
psi	pounds per square inch
rpm	revolutions per minute
sec	Second
TTP	Tactics, Techniques, and Procedures
UCS	unconfined compressive strength
USAF	United States Air Force
yd^3	cubic yard

REPORT DOCUMENTATION PAGE

Form Approved
OMB No. 0704-0188

1. REPORT DATE *(DD-MM-YYYY)*	2. REPORT TYPE	3. DATES COVERED *(From - To)*
February 2021	Final	

4. TITLE AND SUBTITLE

Rapid Airfield Damage Recovery Next Generation Backfill Technologies Comparison Experiment

Technology Comparison Experiment

5a. CONTRACT NUMBER

5b. GRANT NUMBER

5c. PROGRAM ELEMENT NUMBER

6. AUTHOR(S)

Mariely Mejias-Santiago, Lyan Garcia, and Lulu Edwards

5d. PROJECT NUMBER
P246334

5e. TASK NUMBER

5f. WORK UNIT NUMBER

7. PERFORMING ORGANIZATION NAME(S) AND ADDRESS(ES)

Geotechnical and Structures Laboratory
U.S. Army Engineer Research and Development Center
3909 Halls Ferry Road
Vicksburg, MS 39180-6199

8. PERFORMING ORGANIZATION REPORT NUMBER

ERDC/GSL TR-21-2

9. SPONSORING / MONITORING AGENCY NAME(S) AND ADDRESS(ES)

Headquarters, Air Force Civil Engineer Center
Tyndall Air Force Base, FL 32403-5319

10. SPONSOR/MONITOR'S ACRONYM(S)

11. SPONSOR/MONITOR'S REPORT NUMBER(S)

12. DISTRIBUTION / AVAILABILITY STATEMENT

Approved for public release; distribution is unlimited.

13. SUPPLEMENTARY NOTES

14. ABSTRACT

The Rapid Airfield Damage Recovery (RADR) Next Generation Backfill Technology Comparison Experiment was conducted in July 2017 at the East Campus of the U.S. Army Engineer Research and Development Center (ERDC), located in Vicksburg, MS. The experiment evaluated three different crater backfill technologies to compare their performance and develop a technology trade-off analysis. The RADR next generation backfill technologies were compared to the current RADR standard backfill method of flowable fill. Results from this experiment provided useful information on technology rankings and trade-offs. This effort resulted in successful crater backfill solutions that were recommended for further end user evaluation.

15. SUBJECT TERMS

Airfield Damage Repair
Expedient pavement repair
Runways (Aeronautics)—Maintenance and repair
Impact craters
Mechanical stabilization
Chemical stabilization
Expanding polyurethane foam
Cratering
Soil stabilization
Cement stabilization
Geocells
Pavements, Concrete
Polyurethanes

16. SECURITY CLASSIFICATION OF:			17. LIMITATION OF ABSTRACT	18. NUMBER OF PAGES	19a. NAME OF RESPONSIBLE PERSON
a. REPORT	b. ABSTRACT	c. THIS PAGE			19b. TELEPHONE NUMBER *(include area code)*
Unclassified	Unclassified	Unclassified	SAR	92	